Forecasting the Structure and Orientation of Earthbound Coronal Mass Ejections

E.K.J. Kilpua[1], N. Lugaz[2], L. Mays[3], M. Temmer[4]

[1]Department of Physics, University of Helsinki

[2]Space Science Center, Institute for the Study of Earth, Oceans, and Space, University of New Hampshire, Durham, NH, USA

[3]NASA Goddard Space Flight Center, Greenbelt, MD, United States

[4]Institute of Physics, University of Graz, Universitaetsplatz 5, A-8010, Graz, Austria

Accepted Article

This article has been accepted for publication and undergone full peer review but has not been through the copyediting, typesetting, pagination and proofreading process, which may lead to differences between this version and the Version of Record. Please cite this article as doi: 10.1029/2018SW001944

©2019 American Geophysical Union. All Rights Reserved.

Abstract. Coronal Mass Ejections (CMEs) are the key drivers of strong to extreme space weather storms at the Earth that can have drastic consequences for technological systems in space and on ground. The ability of a CME to drive geomagnetic disturbances depends crucially on the magnetic structure of the embedded flux rope, which is thus essential to predict. The current capabilities in forecasting in advance (at least half-a-day before) the geoeffectiveness of a given CME is however severely hampered by the lack of remote-sensing measurements of the magnetic field in the corona and adequate tools to predict how CMEs deform, rotate and deflect during their travel through the coronal and interplanetary space as they interact with the ambient solar wind and other CMEs. These problems can lead not only to over- or underestimation of the severity of a storm, but also to forecasting "misses" and "false alarms" that are particularly difficult for the end-users. In this paper, we discuss the current status and future challenges and prospects related to forecasting of the magnetic structure and orientation of CMEs. We focus both on observational and modeling (first-principle and semi-empirical) based approaches, and discuss the space- and ground-based observations that would be the most optimal for making accurate space weather predictions. We also cover the gaps in our current understanding related to the formation and eruption of the CME flux rope and physical processes that govern its evolution in the variable ambient solar wind background that complicate the forecasting.

Accepted Article

©2019 American Geophysical Union. All Rights Reserved.

Plain-language summary: Coronal Mass Ejections (CMEs) are gigantic magnetized plasma clouds that are frequently expelled from the Sun. Practically all strong and extreme space weather disturbances in the near-Earth space environment are caused by CMEs that propagate in a few days from the Sun to the Earth. Space weather disturbances are related to various harmful effects to modern technology both in space and on ground which can lead to substantial economic losses. Forecasting the CME properties at least half a day before their impact on Earth is thus essential for our society. Our ability to provide accurate predictions of space weather consequences of CMEs is however currently quite modest. The key challenges are related to observational and modeling limitations, and complex evolution CMEs may experience as they propagate from Sun to Earth. This paper discusses the current status and future prospect in forecasting key CME properties using both observations and simulations.

Accepted Article

©2019 American Geophysical Union. All Rights Reserved.

1. Coronal Mass Ejections close to the Sun and in interplanetary space

The largest space weather storms at Earth are caused by coronal mass ejections [CMEs; e.g., *Webb and Howard*, 2012], gigantic plasma clouds that are powered by the complex and ever-changing magnetic field of the Sun. Loop-like magnetic arcades extend from the surface of the Sun to the solar atmosphere and become sheared and twisted by the motion of their footpoints or newly emerging magnetic field. When enough twisting and energization has occurred, the structure may suddenly lose its balance hurling billions of tons of plasma at speeds up to several thousand kilometers per second away from the Sun [e.g., *Forbes*, 2000; *Chen*, 2017].

In remote-sensing observations, CMEs are best seen with white-light coronagraphs. A coronagraph creates an artificial solar eclipse; it blocks the bright solar disk and records sunlight that has scattered from coronal electrons [e.g., *Billings*, 1966]. After their discovery in early 1970s, CMEs were defined as transient and bright features propagating outward through the coronagraph field-of-view [*Munro et al.*, 1979; *Hundhausen et al.*, 1984]. Figure 1 shows a CME observed by the two COR2 coronagraphs [*Howard et al.*, 2008a] onboard Solar TErrestrial RElations Observatory (STEREO) spacecraft. Signatures of CMEs are also observed using a wide range of other wavelengths [e.g., *Howard and DeForest*, 2012], such as Extreme UltraViolet (EUV) emission that comes from various ionization states of heavy ions in the corona and chromosphere, X-rays and radio waves. CMEs are also inherently related to other eruptive phenomena at the Sun, namely solar flares and prominence eruptions; they all often originate nearly simultaneously from the

Accepted Article

©2019 American Geophysical Union. All Rights Reserved.

destabilization of the same large-scale magnetic field structure [e.g., *Zhang et al.*, 2001; *Temmer et al.*, 2008].

After their eruption from the Sun, CMEs propagate through the heliosphere. The fastest CMEs reach the orbit of the Earth (one astronomical unit, AU; 149 597 871 kilometers) in less than a day and slower ones typically in few days [**e.g., *Gopalswamy et al.*, 2001a; *Owens and Cargill*, 2004; *Liu et al.*, 2014**]. When observed in interplanetary space, CMEs are commonly referred to as interplanetary CMEs [ICMEs; e.g., *Kilpua et al.*, 2017] based on characteristic plasma, magnetic field and compositional signatures measured by in-situ instruments. The connection between CMEs and ICMEs has now been unambiguously established with the observations from STEREO heliospheric imagers [*Harrison et al.*, 2005, 2018] starting from the Sun up to 1 AU [*Davis et al.*, 2009; *Möstl et al.*, 2009, 2017].

At the Earth's distance, ICMEs have their radial sizes about 0.2-0.3 AU [e.g., *Gosling et al.*, 1987; *Klein and Burlaga*, 1982; *Jian et al.*, 2006] and on average they propagate past our planet in about one to two days. The magnetic field in ICMEs is typically strong, the magnetic pressure dominates the plasma pressure and the field direction rotates smoothly over a large angle [e.g., *Burlaga et al.*, 1981; *Klein and Burlaga*, 1982]. These are signatures of a magnetic *flux rope*, a configuration where magnetic field lines wind about the central axis.

The flux rope structure is a key factor making ICMEs such powerful drivers of intense space weather storms [e.g., *Gosling et al.*, 1991; *Huttunen et al.*, 2005; *Zhang et al.*, 2007; *Richardson and Cane*, 2012]. Most importantly, flux ropes can provide sustained periods of strongly southward interplanetary magnetic field allowing solar wind energy, plasma and

©2019 American Geophysical Union. All Rights Reserved.

Accepted Article

momentum to enter efficiently the Earth's magnetosphere [e.g., *Dungey*, 1961; *Vasyliunas*, 1975; *Pulkkinen*, 2007].

The interplanetary counterpart of a CME, as shown in Figure 1, is given in Figure 2. This ICME shows a clear field rotation and enhanced magnetic field, featured also by a low ratio of plasma to magnetic pressure (plasma beta). The magnetic field is southward within the flux rope structure and it causes a moderate-level magnetic storm as recorded here by the Dst index which measures the strength of the equatorial ring current [e.g., *Mayaud*, 1980]. The leading shock wave is identified as an abrupt and simultaneous jump of the magnetic field magnitude and plasma parameters, and the sheath by compressed and turbulent plasma and magnetic field [e.g., *Kilpua et al.*, 2017].

Despite decades of research, the accuracy of predicting space weather effects of CMEs in advance (at least half a day) remains rather modest. Direct observations of Earthbound CMEs are typically not available until Lagrangian point L1, about 1.5 million kilometers from the Earth towards the Sun, where it only takes less than an hour for an ICME to reach our planet. The success of long-lead time forecasting thus depends on predicting accurately (1) intrinsic properties of a CME when it erupts from the Sun, and (2) how intrinsic properties change during the propagation from Sun to Earth. As observations in the heliosphere are very limited, step (2) is typically covered by modeling (Figure 3). One of the most critical current issues is that there is no practical method to forecast the magnetic field in CMEs. Space weather forecasts are also very sensitive to variations in the intrinsic CME parameters, including their orientation, direction and magnetic field structure [e.g., *Kay and Gopalswamy*, 2017; *Möstl et al.*, 2018]. Another key challenge is related to the complex and often drastic evolution that CMEs may experience during

Accepted Article

©2019 American Geophysical Union. All Rights Reserved.

their travel through the corona and interplanetary space [e.g., *Manchester et al.*, 2017; *Lugaz et al.*, 2017; *Török et al.*, 2018].

We focus in this paper on the current status of predicting the magnetic structure and orientation of CMEs. We start by discussing societal aspects of CME impacts (Section 2), and then key critical physical aspects of CMEs that make them such challenging phenomena for forecasting space weather (Section 3). In Section 4, we cover the estimations of intrinsic parameters of CMEs and in Section 5, we discuss the modeling of CMEs. Finally, in Section 6, we give key future approaches and prospects for improving CME forecasts. We cover here only those models that are targeted in running (now or in the future) in near-real-time and that focus on modeling the structure and evolution of CMEs. We also do not discuss here solar energetic particles that are another highly important aspect of space weather [*e.g.,*see reviews by *Cane and Lario*, 2006; *Desai and Giacalone*, 2016], but whose forecasting requires largely different approaches than forecasting the consequences of the direct interaction of a CME with the Earth's magnetosphere.

2. Societal Aspect of CMEs

The term "space weather" refers to the variable conditions on the Sun and in the solar wind that can cause disturbances in the near-Earth space, and in the upper part of the Earth's atmosphere and affect the functioning and reliability of technological systems on ground or in space, and endanger human life or health. Direct interaction of solar wind transients with the Earth's magnetosphere, such as CMEs, can lead to significant disturbances in the geomagnetic field, called magnetic storms [*e.g. Gonzalez et al.*, 1994]. They are related to a variety of space weather impacts, such as geomagnetically induced currents that can affect long power grids, oil and gas pipelines at high latitude regions

©2019 American Geophysical Union. All Rights Reserved.

Accepted Article

[e.g., *Pulkkinen*, 2015; *Baker and Lanzerotti*, 2016], and can cause changes in the electric currents and conditions in the ionosphere leading to radio navigation signal disruptions [e.g., *Mendillo and Narvaez*, 2009, 2010]. Intensified ring current built from electrons and ions with energies from few tens of keVs to several hundreds of keVs circling the Earth during magnetic storms can lead to satellite surface charging [e.g., *Ganushkina et al.*, 2015]. In addition, the changing conditions in the upper atmosphere during geomagnetic storms also cause changes in drag experienced by satellites in low-Earth orbits [*Qian and Solomon*, 2012; *Krauss et al.*, 2015; *Guo et al.*, 2016]. All these are harmful effects that have a potential to lead both direct and indirect substantial economical losses [e.g., *Schrijver et al.*, 2015; *Eastwood*, 2017, 2018].

As discussed in the Introduction (Section 1), CMEs are the primary drivers of strong geomagnetic storms and are therefore essential to predict. CMEs are also the only heliospheric structures that can cause extreme space weather storms, such as the famous Carrington storm [*Carrington*, 1859; *Tsurutani et al.*, 2003]. These are very rare events, occurring approximately once in a century [e.g., *Riley et al.*, 2018a, and references therein], but with potential to cause very severe damage to modern technology both in space and on ground [e.g., *Baker et al.*, 2013; *Eastwood*, 2017; *Riley et al.*, 2018a]. An example of an extreme solar and heliospheric event was the 23 July 2012 eruption. This major eruption was composed of two interacting CMEs that decelerated very little during their travel to the Earth orbit, where they were detected directly by the STEREO-A spacecraft. These CMEs caused one of the largest interplanetary magnetic field (IMF) magnitudes recorded at the Earth's distance ($\sim$ 110 nT), and if Earth-bound, could have caused Carrington-

Accepted Article

©2019 American Geophysical Union. All Rights Reserved.

size, or even larger, space weather consequences [e.g., *Baker et al.*, 2013; *Ngwira et al.*, 2013; *Liu et al.*, 2014].

In addition to rare and extreme space weather events, many space weather users are concerned with moderate to severe geomagnetic storms that can cause noticeable disruptions. Space weather forecasts of the north-south component of the IMF (B_Z) during ICME passages are of particular importance for operational agencies and their users. Specifically, many operational centers issue notifications for sustained periods of the southward IMF component is observed, for example when B_Z <-5 nT is sustained for more than 30 minutes. There is a need for producing these type of forecasts well in advance, instead of nowcasts, but there is currently no operational capability to do so.

When compared to terrestrial weather predictions, space weather forecasts have larger errors and shorter lead times. A prediction of a strong geomagnetic storm based on an observation of a fast and bright Earth-directed CME may result in a quiescence ("false alarm") if the magnetic field in the CME points to north [*Tsurutani et al.*, 1992], does not contain a strong magnetic field, or if the CME is channeled away from the Sun-Earth line [e.g., *Möstl et al.*, 2015; *Mays et al.*, 2015a]. In other cases, an ICME and resulting geomagnetic storm may be unexpected, resulting in forecast "misses", such as when a CME is observed remotely to be slow and faint, but the ICME magnetic field is unexpectedly strong enough to drive a storm [e.g., *Tsurutani et al.*, 2004; *Nitta and Mulligan*, 2017]. In other examples, limited coronagraph observations, or narrow and faint CMEs, can result in Earth-directed CMEs being missed in observations [*Webb and Howard*, 2012; *Kilpua et al.*, 2014; *Vourlidas et al.*, 2017] and therefore never forecast. Some CMEs also leave the Sun without any noticeable surface signatures [e.g., *Robbrecht*

©2019 American Geophysical Union. All Rights Reserved.

Accepted Article

et al., 2009; *Nitta and Mulligan*, 2017]. Such "stealth" CMEs are particularly challenging subset for forecasting space weather. Interactions during the propagation can also enhance the geoeffectiveness of a CME [*Liu et al.*, 2014; *Kataoka et al.*, 2015; *Lugaz et al.*, 2017], or a CME originating close to the limb of the Sun may deflect towards Earth [e.g., *Schwenn et al.*, 2005], or an ICME turbulent sheath can drive a storm [e.g., *Huttunen et al.*, 2002; *Lugaz et al.*, 2015a]. Such "false alarms" and "misses" resulting in "surprise storms" are a major concern for space weather predictions and end-users relying on this information.

3. Physical aspects of CMEs

CMEs are a highly complex phenomena. To improve forecasting of their magnetic field structure and orientation, we need a better understanding of the eruption process itself, as well as the interaction with the coronal magnetic field and with solar wind structures and other CMEs when they propagate through interplanetary space. In this section, we discuss the current understanding of the key physical aspects of CMEs and ICMEs and related challenges relevant for space weather forecasting. We start by covering their general properties and morphology, followed by discussing the formation of the magnetic flux rope. We conclude this section by discussing interactions of CMEs with the ambient solar wind and coherence of flux ropes.

3.1. General properties and morphology of CMEs/ICMEs

A huge number of CMEs has been remotely observed over several decades by coronagraphs in space and on ground. For instance, there are now almost 30,000 CMEs in the online catalog `https://cdaw.gsfc.nasa.gov/CME_list/` based on over 20 years of observations by the Large Angle Spectroscopic Coronagraph (LASCO) [*Brueckner et al.*,

©2019 American Geophysical Union. All Rights Reserved.

Accepted Article

1995] onboard the Solar and Heliospheric Observatory (SOHO) spacecraft. Based on these extensive statistics, we now know that the properties of CMEs vary significantly [e.g., *Hundhausen et al.*, 1984; *Yashiro et al.*, 2004; *Thernisien et al.*, 2006; *Yurchyshyn et al.*, 2007; *Shen et al.*, 2013]. For example, the speeds of the CMEs range from a few hundred to several thousands kilometers per second, their widths from less than ten to 360 degrees, and their sources are distributed over a wide range of latitudes.

All CME parameters derived from coronagraph images are however subject to projection effects. This is because the amplitude of the scattering of sunlight from coronal electrons is largest near the plane of the sky [*Hundhausen*, 1993] and because the signal is integrated over the line of sight. Those CMEs that come directly towards the observing spacecraft appear as faint *halos* surrounding the occulting disk of the coronagraph [e.g., *Howard et al.*, 1982]. It is an interesting question whether halo CMEs are truly wider and more violent than other CMEs, or are their distinct properties only due to projection effects [e.g., *Lara et al.*, 2006; *Vršnak et al.*, 2007; *Wang et al.*, 2011; *Shen et al.*, 2013]. According to *Shen et al.* [2013], structured solar wind limits the angular widths of the CMEs to 60 degrees on average. *Kwon et al.* [2015] studied 66 full halo CMEs when STEREO and SOHO were in quadrature configuration and found that in about two-third's of the cases the CME was full halo as seen from all three spacecraft. The authors however noted that often the halo-like appearance was related to an associated extended shock wave that formed a 360 degree "envelope". Unlike the CME flux rope, the shock can propagate through the magnetic field and is not that restricted in size.

Both theoretical and white-light coronagraph observations give a strong support for a flux rope configuration of CMEs. A classical three-part flux rope CME morphology [*Illing*

©2019 American Geophysical Union. All Rights Reserved.

Accepted Article

and Hundhausen, 1985] consists of the cavity, bright core and frontal loop, corresponding to the low plasma beta flux rope, dense prominence material and plasma in coronal loops compressed at the leading edge of the CME, respectively. Recent studies have emphasized a range of morphologies [*Vourlidas et al.*, 2013]; *e.g.*, in addition to the above-described three part structure there are loop-like CMEs that have a bright front, but no cavity nor core, and jet-like CMEs lacking clear substructure. The morphology depends strongly on the viewing angle and is subject to projection effects [*Cremades and Bothmer*, 2004; *Vourlidas et al.*, 2017]. For example, the absence of a cavity is thus likely due to the viewpoint, not due to the lack of the presence of a flux rope.

The CME flux rope is also visible in EUV observations. When viewed from the side, depending on the orientation of the CME, EUV observations reveal either twisted and sheared loops or a cavity [*Zhang et al.*, 2012; *patsourakos et al.*, 2013; *Kliem et al.*, 2014; *Long et al.*, 2018]. The advantage of EUV limb observations is that they extend very low in the corona and thus capture very early evolution of CMEs, showing for example that CME cavities tend to first rise slowly and then expand strongly and rapidly.

In interplanetary space, clear flux rope signatures are present only in about one-third of the ICMEs measured in situ [e.g., *Gosling*, 1990]. The lack of flux rope has been interpreted as being due to deformation of the ICME or due to probing the flux rope far from its center [e.g., *Cane et al.*, 1997; *Cane and Richardson*, 2003; *Huttunen et al.*, 2005; *Jian et al.*, 2006; *Kilpua et al.*, 2011], as in the majority of the cases only single-spacecraft observations of these huge structures are available. The way the magnetic field varies in the flux rope, and thus its geoeffectiveness [see examples *e.g.*, from *Huttunen et al.*, 2005], is dictated by the sign of the magnetic helicity (or chirality), direction of the axial

©2019 American Geophysical Union. All Rights Reserved.

Accepted Article

magnetic field and the orientation of the flux rope axis with respect to the ecliptic plane. Traditionally, these variations are described in terms of "flux rope types" that denote how the north-south magnetic field component rotates within the rope [*Bothmer and Schwenn*, 1998; *Mulligan et al.*, 1998]. If the flux rope axis is perpendicular to the ecliptic plane, **the magnetic field vector measured by the observed spacecraft rotates** in such a way that the field is either northward or southward during the whole passage of the flux rope (as for example in an ICME shown in Figure 2). If the axis is more aligned with the ecliptic plane, the magnetic field vector rotates either from south to north or from north to south.

3.2. Formation of CME flux ropes

While the current consensus regards flux ropes as an integral component of CME eruption, there are still several open questions related to when, where and how they form. The details of this nascent phase has clear implications for estimating the magnetic flux and field structure in CMEs and early evolution of its geometrical and kinetic properties.

Many studies suggest that a flux rope (defined as a structure where magnetic field lines make at least one full turn around the axis of the rope) typically forms in the corona preceding the actual CME onset by magnetic reconnection due to photospheric motions shearing the footpoints of the coronal arcades or due to flux cancellation in emerging active regions [e.g., *Green and Kliem*, 2009; *Amari et al.*, 2011; *Zhang et al.*, 2012; *James et al.*, 2017]. It has been also proposed that flux ropes could form in the convection zone and rise up to the corona by magnetic buoyancy [e.g., *Fan*, 2001; *Martínez-Sykora et al.*, 2008; *Pinto and Brun*, 2013; *Cheung and Isobe*, 2014]. Alternatively, a flux rope could form progressively during the CME eruption when a sheared arcade structure starts to

©2019 American Geophysical Union. All Rights Reserved.

Accepted Article

rise and reconnect, first with the overlying fields and then in the current sheet that forms beneath. This is consistent with the so-called breakout scenario [e.g., *Antiochos et al.*, 1999; *Lynch et al.*, 2004]. Even in the case where the flux rope forms prior to the eruption, its magnetic flux and helicity can increase significantly during the eruption process due to reconnection [e.g., *Qiu et al.*, 2007; *Temmer et al.*, 2017]. In this case, both pre-existing and added magnetic fluxes have to be taken into account when estimating the magnetic flux finally enclosed within the CME.

The CME eruption mechanisms also remain elusive. We summarize here only some key features of this diverse topic that likely includes several different mechanisms whose importance may vary from event to event and that cannot be oversimplified. We guide the interested reader *e.g.*, to recent reviews by *Welsch* [2018] and *Green et al.* [2018] for further information. The studies typically distinguish between the processes that first facilitate the eruption, then trigger an initially stable configuration out of equilibrium and subsequently drive and accelerate the CME away from the Sun.

The addition of poloidal flux increases the magnetic pressure inside the flux rope, initiating an upward magnetic hoop force that leads to the rise of the flux rope [e.g., *Chen*, 1996; *Vršnak*, 2008; *Chen*, 2017]. Some flux ropes also appear to be kinking significantly as they erupt. The kink instability happens when the magnetic field twist in the flux rope exceeds the critical value, $\sim 2-3$ turns, and twist is transformed to the writhe of the flux rope axis [*Török et al.*, 2004]. Both magnetic hoop force and kink instability cause the flux rope to rise to a region where the ambient field decays fast enough to allow it to become torus unstable and escape rapidly from the Sun [e.g., *Kliem and Török*, 2006; **?**; *Zuccarello et al.*, 2014].

Accepted Article

©2019 American Geophysical Union. All Rights Reserved.

Although not necessarily the trigger of the eruption, magnetic reconnection is central for facilitating the eruption. The cutting of magnetic field lines beneath the CME by magnetic reconnection (so-called tether cutting) can both remove the strapping overlying magnetic fields allowing it to rise upward and add poloidal flux to the flux rope. How impulsively a CME is launched depends on the initiation height of the CME, and thus, the magnetic field strength involved in the reconnection process, and tension coming from the overlying field [*Vršnak et al.*, 2004; *Bein et al.*, 2011]. Stealth CMEs (Section 2) are thought to be far less impulsively driven than CMEs which are actively powered by flare-related reconnection processes [*Robbrecht et al.*, 2009; *D'Huys et al.*, 2014]. Rather, they are believed to be launched due to some reconfiguration of the magnetic field in the upper layers of the corona. Their speeds are generally slow, but it is an interesting open question whether or not and how their magnetic structure and further evolution differ from non-stealth CMEs.

3.3. Evolution in interplanetary space

After being launched from the Sun, CMEs start interacting with coronal structures, the ambient solar wind and, sometimes, also with other CMEs. These interactions play a pivotal role in the CME propagation characteristics and in shaping their structure and magnetic field orientation.

The most dramatic evolution of CMEs takes place low in the corona where CMEs are guided by the strong global magnetic field of the Sun and are observed to rotate or get deflected from a radial propagation direction [e.g., *Yurchyshyn et al.*, 2001; *Panasenco et al.*, 2013; *Möstl et al.*, 2015; *Kay and Opher*, 2015]. **The magnetic structure of CMEs is forced to follow the existing pressure gradients and/or magnetic**

©2019 American Geophysical Union. All Rights Reserved.

Accepted Article

forces, from high to low. It may experience magnetic torque affecting different parts of the flux rope leading to rotation. The direction of rotation depends on the chirality of the flux rope; a right-handed flux rope rotates clockwise and a left-handed flux rope rotates counterclockwise [*Lynch et al.*, 2009]. Both statistical and case studies have demonstrated that CMEs can rotate at a rapid rate during their early evolution [e.g., *Lynch et al.*, 2009; *Vourlidas et al.*, 2011; *Thompson et al.*, 2012; *Isavnin et al.*, 2014]: Figure 4 shows a CME on June 16, 2010 from *Vourlidas et al.* [2011] that rotated in the corona with about 60 degrees over a day. Another well studied CME event demonstrating the rapid and complex rotation is a "cartwheel" CME on 9 April 2008 [e.g., *Thompson et al.*, 2012; *Capannolo et al.*, 2017]. The rapid and complex rotations of these CMEs have been attributed to the asymmetries in the reconnection processes during the initiation phase.

Further away from the Sun, magnetic forces diminish rapidly and the evolution of CMEs occurs primarily due to kinematic interactions. While less dramatic, rotations and deflections in interplanetary space cannot be ignored. They can still change significantly the orientation and direction of the flux rope and for some cases even dominate the total change [e.g., *Isavnin et al.*, 2014; *Palmerio et al.*, 2018]. For example, *Good and Forsyth* [2016] reported a case where a flux rope rotated by several tens of degrees while it propagated from Mercury to radially aligned STEREO-B near 1 AU. Especially compression regions associated with stream interaction regions (where fast and slow solar wind regimes meet) or other CMEs, pose obstacles leading to strong deviations from the original propagation direction and changes in the CME kinematics, shape etc. [e.g., *Liu et al.*, 2012; *Temmer et al.*, 2012; *Wang et al.*, 2014; *Möstl et al.*, 2015; *Mishra et al.*, 2015].

Accepted Article

©2019 American Geophysical Union. All Rights Reserved.

For successive CMEs from the same active region, the following CME usually propagates in the path of the preceding one, leading to interaction processes if the following CME is faster than the preceding one. If the fields are in the opposite directions and the Alfvén speed and magnetic field strength are high, significant magnetic reconnection may occur leading to substantial erosion and loss of poloidal flux [e.g., *Dasso et al.*, 2007; *Lugaz et al.*, 2013; *Ruffenach et al.*, 2015]. This also slows down the rate at which CME expands, and with that the propagation speed in radial direction. **In general, the large-scale characteristics of CMEs is a consequence of the competition between the solar wind plasma dynamic pressure and the magnetic forces within the CME flux rope.** On the other hand, poloidal flux might be added to a CME in interplanetary space due to reconnection in the rear of the flux rope, causing an increase of magnetic pressure and speed [e.g., *Manchester et al.*, 2017]. Merging of successive CMEs may lead to a formation of "complex ejecta", single fronts where individual characteristics of eruptions are lost. They can cause extended periods of negative B_z and intensified effects at Earth's magnetosphere [e.g., *Burlaga et al.*, 2002; *Wang et al.*, 2003; *Farrugia et al.*, 2006; *Xie et al.*, 2006; *Lugaz et al.*, 2017].

No merging between two flux ropes occurs if the magnetic fields in the interface are in the same direction or if reconnection is slow. In that case, each flux rope mostly maintains its characteristics, however, their expansion is strongly reduced keeping the magnetic flux very high which may cause enhanced geo-effectiveness compared to isolated CMEs [e.g., *Burlaga et al.*, 1987; *Wang et al.*, 2003; *Lugaz et al.*, 2005; *Farrugia et al.*, 2006; *Xie et al.*, 2006; *Liu et al.*, 2014]. The shock is not restricted by the magnetic field and can propagate through the CMEs and compress the magnetic field within [e.g., *Lugaz et al.*, 2015b]. If

©2019 American Geophysical Union. All Rights Reserved.

Accepted Article

the magnetic field is southward in the ICME, shock compression can substantially enhance geoeffectiveness of the CME [e.g., *Lugaz et al.*, 2015a]. Sometimes CMEs interact already close to the Sun and the merging can be seen in the coronagraph field of view. Such violent "CME cannibalism" [*Gopalswamy et al.*, 2001b] can lead to a particularly large compression of the plasma and field [*Liu et al.*, 2014].

3.4. Coherence of CMEs/ICMEs

The early studies of ICMEs made from multiple vantage points [*Burlaga et al.*, 1990] already suggested them to be huge bent tubes with helical magnetic fields (see Figure 5 from *Zurbuchen and Richardson* [2006]). This picture has now obtained increasing evidence [e.g., *Janvier et al.*, 2013; *Kilpua et al.*, 2017]. It is also found that the magnetic flux rope structure and orientation as derived from in-situ measurements most likely refers to local variations of the global 3D flux rope structure as observed in white-light images [e.g., *Cremades and Bothmer*, 2004; *Möstl et al.*, 2012; *Farrugia et al.*, 2011; *Lugaz et al.*, 2018].

The transformation of an initially coherent CME flux rope to a complex interplanetary ejecta (Section 3.1) remains one of the big open questions in the field [e.g., *Dasso et al.*, 2007; *Richardson and Cane*, 2010; *Kilpua et al.*, 2013]. As discussed in Section 3.3, we now understand that the level of magnetic coherence of an ICME is strongly dependent on its interaction with the ambient solar wind, but the details are not fully resolved. Observations from radially aligned spacecraft give us valuable information on the coherence of the observed structures and the transformation processes. For instance, *Winslow et al.* [2016] showed how interaction of an ICME with a heliospheric plasma sheet increased the complexity of an ICME as it propagated from the orbit of Mercury to the orbit of Earth.

©2019 American Geophysical Union. All Rights Reserved.

Accepted Article

They found a highly turbulent region within the flux rope at STEREO-A that was not observed at MESSENGER.

CME shapes are also distorted by purely kinematic reasons that affect their structure and properties in-situ. The CMEs expand both radially and laterally, *i.e.*, in the direction perpendicular to their radial propagation direction. Observations and simulations show that the lateral expansion is typically significantly larger, resulting in the flattening of CME cross sections, also called as "pancaking" [e.g., *Riley and Crooker*, 2004; *Savani et al.*, 2009; *Isavnin*, 2016]. The interactions affect the expansion, and consequently on how the field and radial dimensions in CMEs evolve [e.g., *Leitner et al.*, 2007; *Gulisano et al.*, 2010].

Recent studies have also started to question the coherence of the CME flux rope on a global scale. Interplanetary space is not homogeneous and can be highly structured due to high speed solar wind streams or preceding CMEs [e.g., *Burlaga et al.*, 2002; *Temmer et al.*, 2011a; *Liu et al.*, 2014; *Temmer et al.*, 2017; *Lugaz et al.*, 2018; *Török et al.*, 2018]. Global changes in the CME shape can occur if the eruption propagates through the solar wind with varying properties influencing different parts of the flux rope loop. These can lead to a gradual flattening of a CME front [*Žic et al.*, 2015] or shaping drastically the CME [*Owens et al.*, 2017a]. *Farrugia et al.* [2011] and *Möstl et al.* [2012] also evidenced the lack of magnetic coherence inside CMEs with case studies showing that the orientation of the flux rope varied considerably along its axis (see Figure 6, which is from *Farrugia et al.* [2011]). In their recent study [*Lugaz et al.*, 2018] found a scale length of the longitudinal magnetic coherence within flux ropes near the Earth orbit to be ~ 0.3

Accepted Article

©2019 American Geophysical Union. All Rights Reserved.

AU for the magnitude of the magnetic field, but significantly less ($\sim$ 0.06–0.12 AU) for the magnetic field components.

4. Intrinsic parameters of CMEs

Determination of the intrinsic CME parameters is pivotal for space weather forecasting. They give the initial estimate whether a certain CME will be geo-effective and the success of modeling of CMEs depends crucially on remote-sensing observations quickly providing realistic input parameters and boundary conditions for physics-based and empirial models. Depending on the model, the input parameters are needed in the low corona or at about 0.1 AU from the Sun (see details from Section 5). The techniques to derive intrinsic properties combine remote-sensing observations, geometrical fitting and data-driven modeling. We discuss first the key geometrical and kinematic CME parameters, and then focus on discussing how to estimate the magnetic field structure in CMEs with various approaches. We conclude this section by contemplating what would be the best place for placing future space weather monitors to guarantee high-quality input parameters.

4.1. Geometric and kinematic parameters in the corona

Information concerning the CME speed and size, direction and orientation is generally obtained from white-light coronagraph observations. These parameters can be derived from single-point coronagraph observations, but as mentioned in Section 3.1, they are subject to the projection effects that get larger the closer to the solar disk center the CME eruption occurs from the view point of the observing spacecraft [*Hundhausen*, 1993; *Michałek et al.*, 2003; *Burkepile et al.*, 2004; *Howard et al.*, 2008b; *Kwon et al.*, 2015]. As most coronagraph observations come from along the Sun-Earth line, projection effects are

©2019 American Geophysical Union. All Rights Reserved.

Accepted Article

a major concern for Earthbound CMEs that typically appear as more or less complete halos.

Observations from large-angle viewpoints minimize the projection effects. If observations from multiple longitudinally separated points are available, they allow getting more reliable parameters [e.g., *Lee et al.*, 2015; *Jang et al.*, 2016] through *e.g.*, three-dimensional (3D) forward modeling [*Thernisien et al.*, 2009] or triangulation [e.g., *Mierla et al.*, 2010; *Rouillard et al.*, 2016]. For example, the graduated cylindrical shell (GCS) model describes the CME as a donut-shaped section attached to two conical legs [croissant-shaped; *Chen et al.*, 1997; *Thernisien et al.*, 2006], see example of the fitting in Figure 7. With this technique, we are able to obtain the 3D speed, size and the tilt angle and propagation direction for flux ropes.

The forward modeling technique can also be used for single spacecraft observations [e.g., *Thernisien et al.*, 2006]. It is, however, much more difficult to fit the CME correctly in this case, in particular if the CME appears as a halo. Single-view CME observations may be also fitted with different cone models, *e.g.* by the ice cream cone model by *Xue et al.* [2005]. The model assumes that the CME front has a spherical shape that is attached to an "ice cream cone". The model provides estimates of the radial speed, angular width and the direction of the CME, but it cannot describe the flux rope characteristic of CMEs (its orientation for example).

Forward modeling is best performed when the CME is already fully evolved in the coronagraph field of view (*e.g.*, distance range of about 15–30 solar radii from the Sun depending on the white-light instrument). Hence, for maximizing the output of the GCS model, one needs to make a compromise with the forecasting lead-time.

©2019 American Geophysical Union. All Rights Reserved.

Accepted Article

4.2. Methods for observing magnetic field directly in CMEs

One of the most significant problems for space weather forecasting is that the magnetic field in CMEs cannot be measured remotely with sufficient accuracy or not at all. The magnetic field in the corona is relatively weak and plasma is extremely hot and tenuous. The emission lines from highly ionized atoms get broadened by thermal and non-thermal processes. As a consequence, measuring the magnetic field using the Zeeman effect in the circularly polarized coronal emission lines is extremely difficult and only a few attempts have successfully estimated the field using this approach [e.g., *Lin et al.*, 2004]. In the photosphere, where the plasma is denser and the field much stronger the Zeeman splitting is a standard technique for measuring the magnetic field magnitude and direction using both ground and space instruments [e.g., *Lagg et al.*, 2017].

Linear polarization measurements employing the Hanle effect can in turn be used for estimating the plane-of-the sky magnetic field direction in the corona. The Hanle effect applies to weaker magnetic fields and it is unaffected by thermal broadening. The Coronal Multi-Channel Polarimeter (COMP) at Sacramento Peak Observatory [*Tomczyk et al.*, 2008] observes the complete polarization state of forbidden emission lines in infrared wavelengths, such as Fe XIII. New facilities have been also suggested, such as COronal Solar Magnetism Observatory (COSMO) [*Tomczyk et al.*, 2016; *Fan et al.*, 2018]. From ground, these measurements are however restricted to the low corona ($< 2R_S$) and for CME cavities seen from the side. It is also not a simple task to routinely obtain the 3D magnetic field structure in CMEs from these measurements, limiting strongly their current usage for space weather forecasting purposes.

©2019 American Geophysical Union. All Rights Reserved.

Accepted Article

Magnetic field magnitudes in CMEs have also been estimated using Faraday rotation with either artificial or natural radio wave sources [*Liu et al.*, 2007; *Howard et al.*, 2016; *Kooi et al.*, 2017] and Type IV gyro-synchronous radio emissions generated by electrons that are trapped gyrating along the magnetic field loops of the CME flux rope [e.g., *Carley et al.*, 2017]. In Faraday rotation, the plane of polarization of light changes as it propagates through magnetized plasma depending on the electron number density and magnetic field magnitude. If the density of a CME is known, *e.g.,* from white-light observations or interplanetary scintillation [e.g., *Bisi et al.*, 2015], one obtains an estimate of the magnetic field integrated along the line of sight. These methods have not yet been applied for near-real time predictions and they cannot be used for all CMEs, either due to lack of continuous observations or due to the fact that not all CMEs produce the required signatures to apply the method. They are nevertheless worthy of further exploration, and can be used in parallel with the other techniques.

4.3. Methods for estimating the intrinsic magnetic field in CMEs through indirect proxies

Several studies have investigated the relationship between solar surface properties and in-situ behavior in order to derive the intrinsic magnetic characteristics of the CME flux rope through statistics [e.g., *Bothmer and Schwenn*, 1998; *Savani et al.*, 2015; *Patsourakos et al.*, 2016; *Palmerio et al.*, 2018] or by case studies [e.g., *Mandrini et al.*, 2005; *Möstl et al.*, 2009; *Palmerio et al.*, 2017; *Temmer et al.*, 2017].

The amount of magnetic flux enclosed in the pre-eruptive structure can be estimated using the flux that was canceled during the active region formation [e.g., *Green et al.*, 2011], while the flux augmented during the eruption can be estimated from magnetograms

©2019 American Geophysical Union. All Rights Reserved.

Accepted Article

using the reconnection area estimations from post-eruptive arcades and/or flare ribbons [e.g., *Qiu et al.*, 2007; *Longcope et al.*, 2007; *Hu et al.*, 2014; *Gopalswamy et al.*, 2017; *Tschernitz et al.*, 2018]. Post-eruption arcades are structures seen in EUV that correspond to recently closed magnetic field beneath the rising CME. These are often outlined by flare ribbons, two parallel structures with enhanced emission related to electrons that are accelerated as a consequence of magnetic restructuring downwards to the more dense atmospheric layers of the Sun where they impact and generate emission in all wavelengths of the electromagnetic spectrum. The above techniques give the flux that roughly equals the poloidal flux in the flux rope. The magnetic field magnitudes in CMEs (or more precisely in the CME sheath) have been estimated using observations of CME shocks with white-light and EUV images [e.g., *Gopalswamy et al.*, 2017; *Bemporad and Mancuso*, 2010]. These techniques use either information of the shock stand-off distance and radius of curvature or derive upstream and downstream plasma parameters that are incorporated to Rankine-Hugoniot equations.

Combination of EUV, H-alpha and X-ray observations and magnetograms can give knowledge of the chirality, axial field direction and axis orientation in CMEs at the time of the eruption [*Martens and Zwaan*, 2001; *Palmerio et al.*, 2017, 2018, and references therein]: Helicity sign can be deduced from various sources, including sigmoids, curls in flare ribbons, and filament threads, and in cases when the CME comes from an emerging active region from "magnetic tongue" signature in magnetograms. Direction of the axial field can be deduced from locating the flux rope's footpoints from EUV dimmings and overlying them to magnetograms. Finally, the orientation of the polarity inversion line over which the erupting flux ropes forms or post-eruptive arcades give a proxy for the

©2019 American Geophysical Union. All Rights Reserved.

Accepted Article

orientation of the axis of the flux ropes. The techniques described above can be applied to several different types of CME, both slow and fast and both those coming from active regions and outside of them [*Palmerio et al.*, 2018]. An example from *Palmerio et al.* [2018] is shown in Figure 8.

Efforts have recently been made to automate the above discussed procedures for space weather forecasting purposes. In the Flux Rope from Eruption Data (FRED) scheme, *Gopalswamy et al.* [2018] determine the poloidal flux in the flux rope using the flare ribbon technique. The assumption of a Lundquist type force-free flux rope [*Lundquist*, 1951; *Burlaga*, 1988] then yields the axial magnetic field strength and the toroidal flux in the flux rope. This now fully constrains the magnetic field in the flux rope that is then combined with the geometric information of the flux rope from the forward modeling fitting to coronagraph images. The Eruptive Event Generator using GibsonLow configuration [EEGGL; *Borovikov et al.*, 2017; *Jin et al.*, 2017] is a tool targeted for finding the input parameters specifically for a Gibson-Low flux rope [*Gibson and Low*, 2000]. In EEGGL, the orientation of the flux rope is deduced from the orientation of the polarity inversion line and the radius is selected such that it encloses the toroidal flux of the model flux rope. The magnetic field chirality is estimated from the hemispheric rule [*Bothmer and Schwenn*, 1998] and the magnetic field strength is obtained from an empirical relationship between the speed of the CME and the amount of reconnected magnetic flux [*Qiu et al.*, 2007; *Hu et al.*, 2014].

Accepted Article

©2019 American Geophysical Union. All Rights Reserved.

4.4. Methods for estimating the intrinsic magnetic field in CMEs through modeling

Data-driven modeling may offer a future method for routine estimation of the intrinsic magnetic structure of CMEs self-consistently for space weather purposes. Full time-dependent MHD simulations are computationally very expensive, and only part of the required data-driven boundary conditions are constrained by the available observations. In addition, properly modeling processes related to coronal heating and solar wind acceleration further complicate the use of MHD-based models. Another option is to use static force-free extrapolations, which neglect the complex thermodynamics taking place in the magnetically dominated low corona. In one of the most general cases, this approach results in the non-linear force free field (NLFFF; e.g., *Wiegelmann and Sakurai* [2012]; *James et al.* [2017]) approximation, where the electric currents are parallel to the magnetic field so that these two are related by a scalar function that varies in space. **Static extrapolations can however give only hints about formation and eruption of the CME magnetic field structures, which are intrinsically dynamic processes.**

One particular NLFFF extrapolation method, the so-called magnetofrictional method [MFM; *Yang et al.*, 1986], can be generalized to a time-dependent modeling approach [e.g., *van Ballegooijen et al.*, 2000], by allowing boundary conditions to evolve in time and relaxing the resulting stressed field at an appropriate rate towards a force-free state, but never reaching it. This time-dependent magnetofrictional method (TMFM) has proven to be able to describe the formation and sometimes also the eruption of the CME magnetic structure [e.g., *Cheung and DeRosa*, 2012; *Fisher et al.*, 2015; *Pomoell et al.*, 2017; *Yardley et al.*, 2018].

Accepted Article

©2019 American Geophysical Union. All Rights Reserved.

The critical boundary condition of the TMFM is the photospheric electric field that is inverted from a time-series of photospheric magnetic field observations. It is possible to use the method with only the line-of-the-sight magnetic field [e.g., *Yardley et al.*, 2018], but recent studies emphasize that the complete constraining of the driving electric field is required for capturing the complex dynamics of the coronal magnetic field consistent with EUV observations. This requires applying photospheric vector magnetograms as well as determining the velocity field by using Dopplergrams and optical flow methods, or alternatively by using carefully constrained ad-hoc assumptions for the velocity-dependent part of the electric field [e.g., *Fisher et al.*, 2010; *Kazachenko et al.*, 2014; *Cheung et al.*, 2015; *Lumme et al.*, 2017].

Since the data-driven CME modeling in the corona largely relies on employing the force-free assumption, vector magnetograms higher up from the chromosphere would in principle offer a more suitable source for the boundary conditions than the currently employed observations from the photosphere [*Wiegelmann et al.*, 2017]. However, the available chromospheric vector magnetogram observations are sparse [*Lagg et al.*, 2017], and they are not yet suitable for routine modeling work. Thus, it remains unclear how much improvement using them would give for the modeling of the intrinsic magnetic field structure in CMEs.

4.5. Optimal locations for space weather monitors

Guaranteeing high-quality knowledge of the intrinsic CME parameters depends crucially on having adequate instrumentation observing the Sun, corona and heliosphere. It is an important question where we should place our future space weather monitors.

©2019 American Geophysical Union. All Rights Reserved.

Accepted Article

Making observations from Earth is typically cheaper and allows possible repairs and updates of the instruments. For some key observations, going to space is the only option as the Earth's atmosphere blocks many frequencies of the sunlight, such as EUV and X-ray frequencies. Photospheric magnetic fields can be observed from Earth with high accuracy and there are several ground-based magnetograms providing continuous observations. Another space weather relevant key observations obtained from ground is the H-alpha. White-light coronagraph observations are also possible from high-altitude ground observatories (*e.g.,* Mauna Loa Solar Observatory). The field of view of the ground based coronagraphs is however smaller and atmospheric scattering can cause significant quality issues, like glaring in images.

In space, the Lagrangian point L1 hosts a number of probes as it is a relatively straightforward place to launch and moreover, it is gravitationally stable. Satellites at L1 perform a small orbital halo motion due to the equal, but opposite, gravitational attraction of the Earth and the Sun. It is also an optimal place to keep space weather monitors. For Earth-bound CMEs, coronagraph observations from L1 strongly limit the determination of CME kinematics due to the maximal projection effects. **L1 is, however, the optimal place for EUV instruments and magnetographs for obtaining detailed observations of Earth-bound CMEs at the time of the eruption for space weather purposes.** First, the quality of magnetograms degrades towards the limb and second, disk EUV signatures are important for deciding where the CME erupted and how it evolved, which can be estimated from the temporal variation of dimming areas [e.g., *Dissauer et al.*, 2018] and/or coronal waves signatures [e.g., *Temmer et al.*, 2011b]. L1 is also a pivotal location for in-situ measurements. While L1 in-situ monitors do not provide long-lead

©2019 American Geophysical Union. All Rights Reserved.

Accepted Article

time forecasting, they are used for now-casting and are of paramount importance for scientific studies of how solar wind couples to the magnetosphere and making the connection between remote-sensing observations and space weather consequences.

Lagrangian points L5 and L4 (Figure 9) would be excellent spots for complementing L1 monitoring. Similar to L1, these points are gravitationally stable, but located at 60° to both sides of the Sun - Earth line. They are particularly well-suited for observing Earth-bound CMEs with coronagraphs and heliospheric imagers [e.g., *Eyles et al.*, 2009; *Harrison et al.*, 2018]. A probe at L5 and L4 would give a side view of Earth-bound CMEs, and the CME parameters could be estimated with a much greater accuracy due to small projection effects (especially kinematics). With simultaneous observations from L1, 3D kinematic CME parameters could be also obtained using multi-spacecraft reconstructions. L5 would have several additional benefits: Evolution of active regions could be followed several days before they rotate to the Earth-impact zone, and magnetograms would provide newer data allowing significantly more realistic modeling of the background solar wind and evolution of active regions [e.g., *Mackay et al.*, 2016; *Petrie et al.*, 2018]. In addition, possible polarimetric observations, using *e.g.,* the far UV range Lyman-α line through the Hanle effect, would allow estimating directly magnetic fields in Earth-bound CMEs [e.g., *Lavraud et al.*, 2016; *Weinzierl et al.*, 2016].

In-situ instruments further towards the Sun from the L1 point would increase forecasting lead-times based on direct measurements. For example, observations made at the orbit of Venus (0.7 AU from the Sun) would increase lead times from an hour to about one day for slow CMEs and for the fastest CMEs from only tens of minutes to several hours. Such observations are however difficult to accomplish on a continuous manner and

©2019 American Geophysical Union. All Rights Reserved.

Accepted Article

CME evolution has to be taken into account. Studies have however demonstrated that observations from the distance of Venus [e.g., *Lindsay et al.*, 1999; *Kubicka et al.*, 2016] or even of Mercury [e.g., *Möstl et al.*, 2018] could provide useful information of CMEs for space weather forecasting purposes. Intriguing suggestions are to use a ring of identical spacecraft circling around the Sun about the distance of 0.7 AU from the Sun [*Ritter et al.*, 2015; *Törmä*, 2016] or the Earth in a diamond like configuration about the distance of 0.9 AU from the Sun [*Cyr et al.*, 2000]. The assumption is that at least one of the satellites would always be close enough to the Sun-Earth line to encounter the Earth-impacting CMEs. In some cases however, conditions in CMEs may change relatively quickly with the increasing distance from the point of the encounter [e.g., *Kilpua et al.*, 2011; *Lugaz et al.*, 2018].

5. Modeling the evolution of CMEs

As coronagraphs are able to give an initial time, direction and speed of CMEs, it has been a natural development to establish tools and methods to determine the interplanetary evolution of CMEs and to forecast their properties and arrival time at L1. Consequently, numerical codes used to investigate CME propagation have been developed ever since the first coronagraphic observations of CMEs, starting in the 1970s [*Dryer*, 1974; *Wu et al.*, 1976].

Most models can be referred to as *first-principle models* as they start from a set of physical equations under given assumptions, such as hydrodynamic (HD), ideal magneto-hydrodynamic (ideal MHD), multi-fluid or multi-species MHD, hybrid (particle treatment of protons and fluid treatment of electrons) or full kinetic (protons and electrons treated as particles). This is complemented by *empirical models*, which are fitted using initial

©2019 American Geophysical Union. All Rights Reserved.

Accepted Article

observations of CMEs (speed, direction, acceleration, etc.) to determine CME properties as they impact the Earth. A last category of forecasting models treats CMEs as a coherent structure to which simplified physical equations can be applied. Hereafter, we review these different approaches that are targeted for (now or in future) forecasting the magnetic field structure of CMEs at 1 AU, their limitations, upcoming challenges and key improvements that can be expected in the near future.

5.1. Initial Conditions for Space Weather modeling

Observations and inputs necessary to perform Sun-to-Earth simulations of CMEs include (1) those required to simulate the background corona, solar wind and IMF and (2) those required to initiate a CME. **It is crucial to know the magnetic field at the base of the corona in order to simulate the background corona and solar wind.** It is typically obtained by extrapolating the photospheric magnetic fields using *e.g.* Potential Field Source Surface (PFSS) modeling, *i.e.,* assuming current-free corona [*e.g., Wiegelmann et al., 2017].* Most current space weather models extend the field to the outer edge of the corona using the Schatten current sheet model and use an empirical formula for the solar wind speed that depends on the magnetic flux tube expansion according to the Wang-Sheeley-Arge (WSA) model [*Wang and Sheeley*, 1990; *Arge and Pizzo*, 2000].

More advanced models solve the MHD equations in the corona to self-consistently derive the coronal configuration, including the magnetic field. Such models also require boundary conditions for the plasma parameters (density, temperature) that can be estimated using certain assumptions [e.g., *Odstrčil and Pizzo*, 1999], or selected through trial-and-error procedure with comparison of the simulations to EUV and white-light observations and to *in situ* measurements [e.g., *Mikić*

©2019 American Geophysical Union. All Rights Reserved.

Accepted Article

et al., 1999; *Riley et al.*, 2001; *Cohen et al.*, 2007]. **The PFSS+WSA model or coronal MHD models can then be coupled (or serve as boundary conditions) for MHD models that focus on the propagation of the solar wind to 1 AU.** Note that full coronal MHD solutions [e.g., *Mikic and Linker*, 1995] are computationally very expensive for space weather forecasting purposes, but recently a combination of uni-dimensional and full MHD model has been suggested [*Pinto and Rouillard*, 2017].

Carrington maps of the magnetic field are often used for space weather forecasting simulations, providing a monthly view of the solar magnetic field which may not reflect rapidly growing or decaying active regions. Recent improvements are Air Force Data Assimilative Photospheric flux Transport (ADAPT) maps that use a photospheric magnetic field flux transport model with various data assimilation techniques [e.g., *Arge et al.*, 2010, 2013; *Henney et al.*, 2012]. The solar polar magnetic field has a strong influence on the amount of open flux in the solar wind as well as the speed of the fast wind also near the ecliptic, but it is not currently measured accurately. Future missions that will go out of the ecliptic, such as Solar Orbiter [*Müller et al.*, 2013] or Solar Polar Imager [*Xiong et al.*, 2017] will provide more accurate measurements of the polar magnetic field and improve dramatically the accuracy of the background solar wind in numerical models.

CMEs are typically initiated using semi-analytical models, such as a spheromak-like "flux rope" as for example the Gibson-Low flux rope or a modified version of the flux rope model of *Titov and Démoulin* [1999], see also *Titov et al.* [2014]. The majority of space weather forecasting models initiates the CME at or around 0.1 AU ($\sim$ 21.5 $R_\odot$), *i.e.,* at a distance where the solar wind is already faster than the fast magnetosonic speed [e.g., see *Odstrčil and Pizzo*, 1999]. Doing so has multiple advantages as well as a

Accepted Article

©2019 American Geophysical Union. All Rights Reserved.

few drawbacks. (1) The solar corona is significantly more computer-intensive to model than the heliosphere, with a timestep typically 1-2 orders of magnitude lower in the inner heliosphere. (2) Starting above the Alfvén surface, there is no "feedback" from the heliosphere into the corona; **it is therefore physically legitimate to fully neglect any feedback from the heliosphere onto the corona when initiating a CME in the inner heliosphere**. (3) The CME speed, size, orientation and direction determined from coronagraphs can be used as input to the model, as discussed earlier in Section 4. Initiating the CME in the upper corona thus allows using observations to capture the results of some of the complex processes occurring in the corona (deflection, acceleration/deceleration, rotation) without capturing the physics itself. The main drawback in initiating CMEs at 0.1 AU is that all current initiation methods rely on relatively simple and "uniform" CME shapes. As such, any deformation and interchange reconnection occurring in the corona and/or any initial complex twist or writhe profile inside the magnetic ejecta will not be reproduced by the simulations. Some space weather forecasting models are also moving towards initiating the CME at the solar surface, which is what is done for most research-based modeling efforts [*Manchester et al.*, 2004; *Chané et al.*, 2005; *Lugaz et al.*, 2007; *Shiota et al.*, 2010; *Shen et al.*, 2013; *Jin et al.*, 2016; *Török et al.*, 2018].

Regardless of where the CME is initiated, its parameters need to be constraint using observational-based techniques (*e.g.*, EEGGL or FRED) or data-driven modeling (see Section 4), or in some cases even using ad-hoc assumptions.

5.2. Modelling CMEs from first principles

Currently, no first-principle model is used in operational setting to forecast CME magnetic fields at 1 AU. The closest to this are ENLIL [*Odstrčil and Pizzo*, 1999; *Odstrcil*

©2019 American Geophysical Union. All Rights Reserved.

Accepted Article

et al., 2002] and EUropean Heliospheric FORecasting Information Asset (EUHFORIA) [*Pomoell and Poedts*, 2018; *Scolini et al.*, 2018], both of which run in real-time with a cone CME model without internal magnetic field and have been tested with flux rope CME models in pseudo-real time settings. The Space-weather-forecast-Usable System Anchored by Numerical Operations and Observations (SUSANOO) [*Shiota et al.*, 2010] and the The Alfven-Wave driven SOlar wind Model (AWSOM-R) + EEGGL[*van der Holst et al.*, 2010, 2014; *Jin et al.*, 2017] run in real-time for the solar wind models and have also been tested with flux rope CME models in pseudo-real time settings.

ENLIL has been the precursor in real-time forecasting, having been run in real-time since the early 2010s at NOAA Space Weather Prediction Center (SWPC) and at the Community Coordinated Modeling Center (CCMC) located at NASA Goddard Space Flight Center (GSFC) [*Zheng et al.*, 2013; *Pizzo et al.*, 2011]. As such, there has been numerous work published on its validation [e.g., see *Taktakishvili et al.*, 2009; *Millward et al.*, 2013; *Wold et al.*, 2018], primarily regarding CME arrival time, and the model has also run several ensemble forecasts [*Lee et al.*, 2013, 2015; *Mays et al.*, 2015b; *Cash et al.*, 2015; *Pizzo et al.*, 2015; *Riley et al.*, 2018b].

ENLIL and EUHFORIA are both 3D MHD codes of the inner heliosphere with an inner boundary usually at 0.1 AU (ı.e., about 21.5 $R_{\odot}$). They both use the WSA model with daily updated magnetograms to generate the ADAPT maps to provide the plasma parameters to drive the heliospheric model. As mentioned above, these models are currently run with a cone-model CME [e.g., *Xie et al.*, 2004] in real-time, but recently simulations with a flux rope model have been presented at international conferences [e.g., *Pomoell et al.*, 2017; *Odstrcil et al.*, 2018; *Odstrcil*, 2018; *Verbeke et al.*, 2018].

©2019 American Geophysical Union. All Rights Reserved.

Accepted Article

SUSANOO is a 3-D MHD code developed by *Shiota and Kataoka* [2016]. In it, CMEs are initiated at 30 $R_\odot$ with a spheromak-like flux rope. The CME speed, onset time and position are obtained from remote-sensing observations. The CME is assumed to be of high density and constant-pressure throughout. For the tilt of the ejecta magnetic field, the Hale-Nicholson relation for polarity is used. The magnetic flux inside the CME is a function of the flare class and all CMEs are assumed to be of the same radial and angular size at 30 $R_\odot$.

The solar wind model AWSOM-R in AWSOM-R+EEGGL in turn starts from the surface of the Sun. The Block-Adaptive-Tree-Solarwind-Roe-Upwind-Scheme (BATS-R-US) is used for solving the 3D MHD equations [*van der Holst et al.*, 2014]. The EEGGL scheme described in Section 4.3 provides the input parameters for a Gibson-Low flux rope that is inserted in the AWSOM-R model.

It is likely that the accuracy of the forecasts with flux rope CMEs will strongly depend on the initial conditions chosen for the CMEs, as is the case for simulations performed for basic research and highlighted through ensemble forecasting. Therefore, a slightly more distant prospect, in the 5 to 20 years range, is the development of real-time forecasting with more accurate CME eruption models. This might be done by obtaining an eruption from an initially quasi-stable flux rope [*Amari et al.*, 2014; *Török et al.*, 2018], self-consistently using a static NLFFF model [*James et al.*, 2017; *Savcheva et al.*, 2017], time-dependent magnetofrictional method (TMFM) [e.g., *Cheung and DeRosa*, 2012; *Pomoell et al.*, 2017; *Pagano et al.*, 2018, and see Section 4.4] or full MHD simulations [e.g., *Chen*, 2011; *Jiang et al.*, 2016], with a flux emergence model partially coupled to the coronal model [*Roussev et al.*, 2012] or with a fully coupled corona-flux emergence code [*Fang et al.*, 2010]. These

©2019 American Geophysical Union. All Rights Reserved.

Accepted Article

are presented in approximate order of complexity. These approaches however have some issues with detailed boundary conditions they require (vector magnetograms, EUV and X-Ray images, etc.) and being still too long to run in real-time.

In the longer term, developing models for real-time forecasting that go beyond MHD will be necessary, as MHD models do a very poor job at capturing the complexity of the CME sheath, and a relatively poor job at accurately incorporating magnetic reconnection, which is central for CME erosion and CME-CME interactions. Coupled MHD and kinetic or hybrid models will be a more realistic solution, due to the limitations in the machine size for real-time modeling, than full kinetic models. Such models are currently being developed [*Daldorff et al.*, 2014; *Tóth et al.*, 2016; *Makwana et al.*, 2018], although they have not been used yet for the solar corona.

5.3. Modeling of CMEs using semi-empirical approaches

Semi-empirical models are also powerful tools for forecasting in advance the structure and properties of Earth-impacting CMEs. They produce synthetic estimates of the in-situ parameters, including magnetic field vectors at L1 (or another selected location) that can then be used for forecasting purposes. These models are quick to use and computationally efficient, but they typically capture only a subset of deformation effects CMEs may experience in interplanetary space.

Examples of recent semi-empirical models targeted for predicting the magnetic structure and/or orientation of CMEs are Bz4cast (based on works in *Savani et al.* [2015] and *Savani et al.* [2017]), 3DCORE [*Möstl et al.*, 2018], The Forecasting a CMEs Altered Trajectory (ForeCAT) + FIDO [*Kay et al.*, 2013, 2017], Fri3D [*Isavnin*, 2016], and Helicity-CME [*Patsourakos et al.*, 2016; *Patsourakos and Georgoulis*, 2017]. Efforts have also been made

©2019 American Geophysical Union. All Rights Reserved.

Accepted Article

using Interplanetary Scintillation (IPS) tomographic analysis, but predictions for large out-of-ecliptic fields are particularly challenging [*Jackson et al.*, 2018].

Nearly all semi-empirical models assume that CMEs have a flux rope topology. The common approach is to estimate the intrinsic magnetic parameters in CMEs from indirect solar observations as discussed in Section 4 or from known statistical dependences, *e.g.* using the hemispheric rule for the magnetic helicity sign by *Bothmer and Schwenn* [1998] or using the relationship between the magnetic flux and the speed of the CME [*Qiu et al.*, 2007]. *Patsourakos et al.* [2016] used instead a different approach; they applied three different methods based on magetograms to calculate the magnetic helicities in flux ropes in the low corona and then force-free and non-force free flux rope models to estimate the magnetic structure of the CME at 13 solar radii.

The propagation direction, speed and geometrical flux rope parameters are typically obtained from the GCS forward modeling. Then, the CME flux rope is propagated in interplanetary space under certain assumptions, *e.g.,* assuming a self similar evolution and drag-based deceleration/acceleration [see *e.g.*, *Vršnak et al.*, 2004]. The magnetic fields are extrapolated using the power law dependence with the heliospheric distance [see *e.g.*, *Leitner et al.*, 2007].

The assumption of **the magnetic configuration of the CME** varies between the models. For example, in 3DCORE the model CME envelope is a torus with 2.5-dimensional circular cross section and a uniform "Gold-Hoyle" twist, while Fri3D model defines a fully analytic 3D flux rope shell and populates it with a magnetic field. Fri3D takes into account all major deformation the CME is expected to experience, including the front flattening and pancaking and skewing of the CME flux rope loop due to the

Accepted Article

©2019 American Geophysical Union. All Rights Reserved.

rotation of the Sun. The model has relatively large number of free parameters, but the uniqueness of the solution is estimated to be relatively robust, possibly due to strong constraints from the geometrical fitting.

The ForeCAT model estimates the rotation and deflections in the corona by defining both magnetic tension and magnetic pressure gradient forces from the PFSS model on a CME described as a rigid torus. The results are used as the input to FIDO, which assumes the force-free flux rope model by *Burlaga* [1988] and self-similar expansion. In the current version of the model the magnetic helicity sign is obtained from the hemispheric rule and the magnetic field strength is an unconstrained parameter. In the future, more realistic estimates could be obtained from previously described techniques based on indirect observations proxies, FRED and EEGGL techniques or from data-driven modeling.

Within the class of semi-empirical models, models purely based on statistics of past events, past data and pattern recognition [e.g., *Riley et al.*, 2017; *Owens et al.*, 2017b; *Camporeale et al.*, 2017] or neural networks [e.g., *Yang et al.*, 2018] have been proposed or are currently being developed. These models have shown promising results for the prediction of the solar wind speed or density at 1 AU, but their appropriateness for forecasting the magnetic field inside CMEs and CME-driven shocks/sheaths is yet unproven. At the core of this issue is the fact that, in the 25 years with *Wind* measurements, there have only been about 400 CMEs measured and less than 150 CME-driven intense storms. This represents 1-5% of all time periods and is a relatively small number on which to base a pattern recognition technique. **A recently proposed technique focuses only on forecasting southward magnetic fields following a shock using pattern recognition, as $\sim$ 20% of fast-forward shocks are followed by strong, long-duration**

©2019 American Geophysical Union. All Rights Reserved.

Accepted Article

southward magnetic fields [*Salman*, 2018]. This issue is exacerbated for extreme events, which typically appear to be due to a set of unusual circumstances with multiple CMEs and solar wind streams often involved. This issue applies more generally for all semi-empirical models.

5.4. Model validation

Model validation is important for advancing our scientific understanding, aiding in model development, and for forecasting. Generally, for assessing IMF model outputs, the community has been performing time series comparisons of model output to observations for each magnetic field component, and sometimes aggregating this to an overall assessment of predicting all of the components. Usually the simulated time series output is time shifted to the front end of the observed ICME. *Kay and Gopalswamy* [2017] assess the quality of FIDO model output by computing the vector magnitude of the average hourly error weighted by the average hourly observed total magnetic field strength. Zero represents a perfect score, one, when the model predicts zero or twice the observation values, and two, results when the model prediction is opposite sign to the observation. With this method, a combined metric is derived such that too much emphasis is not placed on small components. Applying this metric to their sample of 45 CMEs modeled with FORECAT+FIDO yielded 0.72±0.2.

As another example, *Savani et al.* [2017] use the magnetic field model output from the Bothmer-Schwenn scheme to produce a Kp model prediction. Different thresholds were then applied to the continuous Kp model output and compared to observations in order to produce a contingency table for each "event". They found a True Skill Statistic ranging from 0.33 to 0.58 depending on the threshold used, for eight ICME events. Current

©2019 American Geophysical Union. All Rights Reserved.

Accepted Article

validation items, including coordinates, thresholds and related durations, time cadence, and multiple or combined skill scores, are also actively considered by the IMF Bz Working Team that is one team within the CCMC facilitated International Forum for Space Weather Capabilities Assessment[1]. Each working team is made up by the community and their goals are to define metrics and assess the current state of space weather modeling. Note that for many first-principle models of the IMF, model validation has not been performed beyond a handful of case studies, and more effort is needed here.

Ensemble modeling is useful to quantify prediction uncertainties and determine forecast confidence. An overall single forecast can be derived from multiple ensemble member forecasts, however ensembles also give information about possible scenarios and therefore also provide a probabilistic forecast. Space weather forecasters have emphasized the importance of having an uncertainty associated with model outputs to the scientific community, and ensembles would provide this. *Mays et al.* [2015b] discuss ensemble CME modeling and validation in the context of predicting CME arrival time and Kp specifically using the WSA–ENLIL+Cone model. Similar to the concept of ensemble modeling for CME arrival time, ensemble IMF modeling could also provide a probabilistic Kp, or other geomagnetic index or parameter, forecast in addition to an ensemble IMF forecast. Having an ensemble of IMF model output would also bypass the issue of needing to convert deterministic outputs to probabilistic, in order to access probabilistic metrics.

Currently there are very few ensemble models (FIDO is one example) producing outputs for the magnetic field components related to ICMEs, but in principle this is possible with many existing models. Alternatively, outputs from multiple models can also be used as individual members to create an ensemble of multiple models. One such ensemble forecast

©2019 American Geophysical Union. All Rights Reserved.

Accepted Article

could be produced by the CCMC's Bz Scoreboard project[2], currently in early planning phases, and is led by NASA GSFC, Predictive Science, and CCMC. In general, the idea behind CCMC's scoreboards is to allow the testing of predictive capabilities before event onset and the community is encouraged to participate in these efforts either in scoreboard planning, providing advice, contributing forecasts, validating results, or viewing forecasts.

6. Summary of the current status and future outlook

An increasing demand for accurate long-lead time space weather forecasts by end-users calls upon the science community to refine our prediction techniques. Being the key drivers of strong and extreme geomagnetic storms and an important contributor to smaller disturbances as well, CMEs are at the focus of solar-terrestrial research and a considerable effort has been placed on predicting their properties in the near-Earth solar wind. The fastest CMEs hurl to the Earth in less than a day, and thus, predictions need to be done quickly and they have to rely on observations taken as close to the Sun as possible to maximize the lead-times. We have here focused in particular on summarizing the current status and challenges related to predicting the magnetic structures and orientation of CMEs.

An evident challenge in forecasting is the variability of CMEs, the coronal environment in which they are born, and the background solar wind into which they propagate. The initial widths, geometry, speeds and orientations of CMEs vary considerably from case to case and also their internal magnetic field structure. Depending on the ambient coronal field structure and the solar wind they encounter ahead and behind can change the intrinsic properties of CMEs drastically and uniquely.

Accepted Article

©2019 American Geophysical Union. All Rights Reserved.

As discussed in this paper there is currently no first-principle forecasting model running in real-time with a flux rope CME. As initial studies have already been performed, we can expect that in the near-future operational space weather simulations run with spheromak or flux rope CMEs (inserted at 20-30 $R_{\odot}$ for ENLIL, EUFHORIA and SUSANOO and at or near the solar surface for AWSOM-R + EEGGL). When successful, this should provide a substantial improvement to forecasting accuracy as it allows predicting the magnetic field structure of CMEs as they arrive at the Earth and would reduce in particular the number of geomagnetic storm "false alarms". Semi-empirical models are another powerful approach in predicting the magnetic structure of Earthbound CMEs, and some capture also the rotation and deflections during the propagation. They however typically take into account only a limited number of deformations CMEs can experience in interplanetary space and cannot account very realistically the structured and changing solar wind background, nor the interactions between multiple CMEs. Furthermore, not all aspects relevant for space weather forecasting can be captured by magnetohydrodynamic and semi-empirical modeling approaches. To model complex processes such as details of CME-CME interactions and evolution of CME sheath region likely requires kinetic or hybrid simulations.

This increasing sophistication of forecasting approaches requires that realistic input parameters/boundary conditions are provided to constrain the flux rope models and for the background solar wind modeling. The importance of providing information on 3D kinematic and geometric properties of CMEs in near-real time and to gather that information in catalogs, has been emphasized in the community, as well as the need to revise our concepts of CME morphology in light of the latest results. Due to the observational

©2019 American Geophysical Union. All Rights Reserved.

Accepted Article

limitations and the complexity of the magnetic field involved in a CME event during its initiation, clearly, predicting realistically of their intrinsic magnetic structure, either with observational techniques or using data-driven modeling, is a major future challenge. Considering these current uncertainties in the initial conditions, it is also a major unresolved question what are the advantages of full 3-D simulations for forecasting isolated (*i.e.*, non-interacting) CMEs as opposed to semi-empirical approaches.

Guaranteeing continuous monitoring of the Sun and the corona with sufficient instrumentations is therefore crucial for space weather forecasting. Projection effects are a severe concern if white-light observations are only available from L1, and for constraining 3D CME properties multi-point observations are an indispensable necessity. An optimal situation for long-lead time forecasting would be having space probes with remote-sensing instrumentations both at L1 and L5. This would allow getting both head-on and side view of Earth-impacting CMEs, geometric 3D reconstructions, and following the evolution of regions on the Sun well in advance while also getting a good view of the source region at the time of the eruption. From L5, CMEs could also be followed with heliospheric imagers at larger distances, allowing to revise forecasting as the eruption propagates. There are indeed active plans for a space weather mission to L5 [e.g., *Vourlidas*, 2015; *Gibney*, 2017].

One of the biggest future challenges is also to capture all complexities in the evolution of a CME over huge spatial distances from Sun to Earth, in particular rotation and deflection and changes in properties due to interactions with the ambient solar wind and other CMEs. A key focus should be on the evolution in the low corona, where the most drastic changes are expected due to strong magnetic forces.

©2019 American Geophysical Union. All Rights Reserved.

Accepted Article

To conclude, accurate long-lead time forecasting of CMEs structure and orientation is an extremely challenging topic that requires significant future improvements related to the modeling, observational techniques and physical understanding of CMEs and related key processes. Guaranteeing continuation of L1 and ground observations of CMEs is paramount as well as improving the current observational network, *e.g.*, with an L5 space weather probe. To move forward, it is also critical to discuss actively on the optimal combination of models (first principle and semi-empirical) and techniques to constrain flux rope parameters to obtain realistic predictions of CME properties as they impact the Earth. This evidently requires active collaboration across solar and interplanetary, and numerical and empirical communities, as well as between researchers and forecasters.

7. Plain Language Summary (BOXED TEXT)

7.1. Coronal mass ejections and space weather

Our modern society has become increasingly dependent on technology in space and on ground that solar eruptions can damage. The strongest of such space weather storms are driven by Coronal Mass Ejections (CMEs) - enormous eruptions of charged material from the outermost layer of the solar atmosphere –the corona. CMEs occur from once to several times per day depending on the phase of the solar activity cycle, and when Earth-directed, they typically reach our planet within a few days. Forecasts need to be made quickly using imaging of the Sun and simulations. The ability of CMEs to drive significant space weather storms stems from their specific magnetic configuration; CMEs are thought to consist of huge and bending helical flux ropes where the magnetic field is enhanced and the field direction rotates smoothly. To forecast CME properties as

Accepted Article

©2019 American Geophysical Union. All Rights Reserved.

they arrive at Earth we need to estimate accurately both intrinsic properties of CMEs as they erupt from the Sun and how they change in the corona and interplanetary space.

7.2. Challenging aspects

The reliability of long-lead time space weather forecasting of CMEs is still very modest. The key challenges are the variability of CMEs and solar wind background they propagate into and lack some crucial observations, most importantly the magnetic field in the corona and continuous multi-point observations allowing reconstructions of CMEs geometric and kinematic properties (size, speed, orientation, propagation direction). Modeling of CMEs faces also several challenges related to the complexity and variability of CMEs and related physical processes, computer efficiency and issues with observations providing boundary conditions. The spatial scales involved are huge and CMEs may deform, deflect and rotate dramatically as they interact with the other CMEs and the ambient solar wind. All these changes need to be captured by successful forecasting.

7.3. Summary of the current status

Operational space weather forecasts are currently primarily made using heliospheric magnetohydrodynamic models. Their key missing element is the magnetic flux rope CME, which severely limits their forecasting accuracy. There are several on-going efforts to include flux ropes (US ENLIL, European EUHFORIA), but none of them is yet routinely able to predict magnetic field in CMEs. Another option is to use semi-empirical CME flux rope models. They are computer efficient, but limited in their capability to describe the evolution and interactions of CMEs. The accuracy of all these forecasting models depends crucially on initial con-

Accepted Article

©2019 American Geophysical Union. All Rights Reserved.

ditions chosen for the CMEs, and also realistic description of the background solar wind. The geometric and kinematic CME parameters in the corona (covering approximately the first 5-10% of the CMEs Sun-to-Earth journey) can be quickly obtained from white-light coronal images using single or multi-spacecraft reconstructions. The magnetic properties can be estimated using indirect proxies, but it is not yet rigorously evaluated how realistically they can constrain CME flux ropes for space weather forecasting purposes. Many of these techniques are also based on relatively strong assumptions and they are also subject to issues with the observations. While several physical processes have been identified that can deform, deflect and rotate CMEs, they are not well captured by most of the current forecasting methods. There are also gaps related to our physical knowledge of CMEs, e.g., it is not yet clear how CME flux ropes form and erupt. Recent studies also suggest that the flux rope configuration may not always be coherent on a global scale. Significant deviations can occur both due to temporal evolution and as the CME propagates through a non-uniform solar wind.

7.4. Future outlook

An important near-future improvement will be running heliospheric magnetohydrodynamical models with flux rope CMEs. It is thus paramount to improve also the realism of intrinsic CME parameters to constraint the flux ropes. For this, high-quality remote-sensing observations are pivotal from upstream of the Earth and from the ground that in the optimal case would be complemented by observations from the side, e.g., with a space weather probe at the gravitationally stable Lagrangian point L5. An L5 probe would also allow following active regions on the Sun several days before eruption and tracking CMEs in the inner heliosphere with white-light heliospheric imaging. An intriguing future way

©2019 American Geophysical Union. All Rights Reserved.

Accepted Article

to get realistic and self-consistent information of the magnetic field structure in CMEs in the corona for space weather forecasting is through data-driven modelling using observations from the surface of the Sun, the photosphere as boundary conditions. In the more distant future, first-principle space weather models could be coupled all the way from the surface of the Sun to Earth. **Forecasting realistically interactions between multiple CMEs and between the CME and the ambient solar wind, as well as the properties of turbulent CME sheath regions might require kinetic modelling that is computationally a very expensive approach.** Other more distant future possibilities include forecasting methods based on statistics, pattern recognition and neural networks. In summary, future efforts to improve forecasting of CME structure and evolution need advancing both observational and modeling techniques and also providing sufficient observations and improving our understanding of physical foundations of CMEs.

Acknowledgments. M.T. acknowledges the support by the FFG/ASAP Program under grant no. 859729 (SWAMI). EK acknowledges the European Research Council (ERC) under the European Union's Horizon 2020 Research and Innovation Programme Project SolMAG 4100103, and Academy of Finland Project 1310445. The results presented in here have been achieved under the framework of the Finnish Centre of Excellence in Research of Sustainable Space (Academy of Finland grant number 1312390), which we gratefully acknowledge. NL acknowledges the support from NASA grant NNX15AB87G and NSF grant AGS-1435785. EK acknowledges Jens Pomoell and Erkka Lumme for discussions about data-driven modeling. All the data used are listed in the references.

Accepted Article

©2019 American Geophysical Union. All Rights Reserved.

Notes

1. https://ccmc.gsfc.nasa.gov/assessment/

2. https://ccmc.gsfc.nasa.gov/challenges/bz.php

References

Amari, T., J.-J. Aly, J.-F. Luciani, Z. Mikic, and J. Linker, Coronal Mass Ejection Initiation by Converging Photospheric Flows: Toward a Realistic Model, *Astrophys. J.*, *742*, L27, doi:10.1088/2041-8205/742/2/L27, 2011.

Amari, T., A. Canou, and J.-J. Aly, Characterizing and predicting the magnetic environment leading to solar eruptions, *Nature*, *514*, 465–469, doi:10.1038/nature13815, 2014.

Antiochos, S. K., C. R. DeVore, and J. A. Klimchuk, A Model for Solar Coronal Mass Ejections, *Astrophys. J.*, *510*, 485–493, doi:10.1086/306563, 1999.

Arge, C. N., and V. J. Pizzo, Improvement in the prediction of solar wind conditions using near-real time solar magnetic field updates, *J. Geophys. Res.,* , *105*, 10,465–10,480, doi:10.1029/1999JA000262, 2000.

Arge, C. N., C. J. Henney, J. Koller, C. R. Compeau, S. Young, D. MacKenzie, A. Fay, and J. W. Harvey, Air Force Data Assimilative Photospheric Flux Transport (ADAPT) Model, *Twelfth International Solar Wind Conference*, *1216*, 343–346, doi:10.1063/1.3395870, 2010.

Arge, C. N., C. J. Henney, I. G. Hernandez, W. A. Toussaint, J. Koller, and H. C. Godinez, Modeling the corona and solar wind using ADAPT maps that include far-side observations, *Solar Wind 13*, *1539*, 11–14, doi:10.1063/1.4810977, 2013.

©2019 American Geophysical Union. All Rights Reserved.

Accepted Article

Baker, D. N., and L. J. Lanzerotti, Resource Letter SW1: Space Weather, *American J. Phys.*, *84*, 166–180, doi:10.1119/1.4938403, 2016.

Baker, D. N., X. Li, A. Pulkkinen, C. M. Ngwira, M. L. Mays, A. B. Galvin, and K. D. C. Simunac, A major solar eruptive event in July 2012: Defining extreme space weather scenarios, *Space Weather*, *11*, 585–591, doi:10.1002/swe.20097, 2013.

Bein, B. M., S. Berkebile-Stoiser, A. M. Veronig, M. Temmer, N. Muhr, I. Kienreich, D. Utz, and B. Vršnak, Impulsive Acceleration of Coronal Mass Ejections. I. Statistics and Coronal Mass Ejection Source Region Characteristics, *Astrophys. J.*, *738*, 191, doi:10.1088/0004-637X/738/2/191, 2011.

Bemporad, A., and S. Mancuso, First Complete Determination of Plasma Physical Parameters Across a Coronal Mass Ejection-driven Shock, *Astrophys. J.*, *720*, 130–143, doi:10.1088/0004-637X/720/1/130, 2010.

Billings, D. E., *A guide to the solar corona*, 1966.

Bisi, M. M., J. Americo Gonzalez-Esparza, B. V. Jackson, M. Tokumaru, and J. Leibacher, Preface: Radio Heliophysics: Science and Forecasting, *Sol. Phys.*, *290*, 2393–2396, doi:10.1007/s11207-015-0784-y, 2015.

Borovikov, D., I. V. Sokolov, W. B. Manchester, M. Jin, and T. I. Gombosi, Eruptive event generator based on the Gibson-Low magnetic configuration, *Journal of Geophysical Research (Space Physics)*, *122*, 7979–7984, doi:10.1002/2017JA024304, 2017.

Bothmer, V., and R. Schwenn, The structure and origin of magnetic clouds in the solar wind, *Annales Geophysicae*, *16*, 1–24, doi:10.1007/s00585-997-0001-x, 1998.

Brueckner, G. E., et al., The Large Angle Spectroscopic Coronagraph (LASCO), *Sol. Phys.*, *162*, 357–402, doi:10.1007/BF00733434, 1995.

Accepted Article

©2019 American Geophysical Union. All Rights Reserved.

Burkepile, J. T., A. J. Hundhausen, A. L. Stanger, O. C. St. Cyr, and J. A. Seiden, Role of projection effects on solar coronal mass ejection properties: 1. A study of CMEs associated with limb activity, *Journal of Geophysical Research (Space Physics)*, *109*, A03103, doi:10.1029/2003JA010149, 2004.

Burlaga, L., E. Sittler, F. Mariani, and R. Schwenn, Magnetic loop behind an interplanetary shock - Voyager, Helios, and IMP 8 observations, *J. Geophys. Res.*, *86*, 6673–6684, doi:10.1029/JA086iA08p06673, 1981.

Burlaga, L. F., Magnetic clouds and force-free fields with constant alpha, *J. Geophys. Res.*, *93*, 7217–7224, doi:10.1029/JA093iA07p07217, 1988.

Burlaga, L. F., K. W. Behannon, and L. W. Klein, Compound streams, magnetic clouds, and major geomagnetic storms, *J. Geophys. Res.*, *92*, 5725–5734, doi:10.1029/JA092iA06p05725, 1987.

Burlaga, L. F., R. P. Lepping, and J. A. Jones, Global configuration of a magnetic cloud, *Washington DC American Geophysical Union Geophysical Monograph Series*, *58*, 373–377, doi:10.1029/GM058p0373, 1990.

Burlaga, L. F., S. P. Plunkett, and O. C. St. Cyr, Successive CMEs and complex ejecta, *Journal of Geophysical Research (Space Physics)*, *107*, 1266, doi:10.1029/2001JA000255, 2002.

Camporeale, E., A. Carè, and J. E. Borovsky, Classification of Solar Wind With Machine Learning, *Journal of Geophysical Research (Space Physics)*, *122*, 10, doi:10.1002/2017JA024383, 2017.

Cane, H. V., and D. Lario, An Introduction to CMEs and Energetic Particles, *Space Sci. Rev.*, *123*, 45–56, doi:10.1007/s11214-006-9011-3, 2006.

©2019 American Geophysical Union. All Rights Reserved.

Accepted Article

Cane, H. V., and I. G. Richardson, Interplanetary coronal mass ejections in the near-Earth solar wind during 1996–2002, *J. Geophys. Res.*, *108*, 1156, doi:10.1029/2002JA009817, 2003.

Cane, H. V., I. G. Richardson, and G. Wibberenz, Helios 1 and 2 observations of particle decreases, ejecta, and magnetic clouds, *J. Geophys. Res.*, *102*, 7075–7086, doi:10.1029/97JA00149, 1997.

Capannolo, L., M. Opher, C. Kay, and E. Landi, The Deflection of the Cartwheel CME: ForeCAT Results, *Astrophys. J.*, *839*, 37, doi:10.3847/1538-4357/aa6a16, 2017.

Carley, E. P., N. Vilmer, P. J. A. Simões, and B. Ó Fearraigh, Estimation of a coronal mass ejection magnetic field strength using radio observations of gyrosynchrotron radiation, *Astron. Astrophys.*, *608*, A137, doi:10.1051/0004-6361/201731368, 2017.

Carrington, R. C., Description of a Singular Appearance seen in the Sun on September 1, 1859, *Monthly Notices of the Royal Astronomical Society*, *20*, 13–15, doi:10.1093/mnras/20.1.13, 1859.

Cash, M. D., D. A. Biesecker, V. Pizzo, C. A. de Koning, G. Millward, C. N. Arge, C. J. Henney, and D. Odstrcil, Ensemble Modeling of the 23 July 2012 Coronal Mass Ejection, *Space Weather*, *13*, 611–625, doi:10.1002/2015SW001232, 2015.

Chané, E., C. Jacobs, B. van der Holst, S. Poedts, and D. Kimpe, On the effect of the initial magnetic polarity and of the background wind on the evolution of CME shocks, *Astron. & Astrophys.*, *432*, 331–339, doi:10.1051/0004-6361:20042005, 2005.

Chen, J., Theory of prominence eruption and propagation: Interplanetary consequences, *J. Geophys. Res.*, *101*, 27,499–27,520, doi:10.1029/96JA02644, 1996.

Chen, J., Physics of erupting solar flux ropes: Coronal mass ejections (CMEs), Recent

Accepted Article

©2019 American Geophysical Union. All Rights Reserved.

advances in theory and observation, *Physics of Plasmas*, *24*(9), 090501, doi:10.1063/1.4993929, 2017.

Chen, J., et al., Evidence of an Erupting Magnetic Flux Rope: LASCO Coronal Mass Ejection of 1997 April 13, *Astrophys. J. Lett.*, *490*, L191–L194, doi:10.1086/311029, 1997.

Chen, P. F., Coronal Mass Ejections: Models and Their Observational Basis, *Living Reviews in Solar Physics*, *8*, 1, doi:10.12942/lrsp-2011-1, 2011.

Cheung, M. C. M., and M. L. DeRosa, A Method for Data-driven Simulations of Evolving Solar Active Regions, *Astrophys. J.*, *757*, 147, doi:10.1088/0004-637X/757/2/147, 2012.

Cheung, M. C. M., and H. Isobe, Flux Emergence (Theory), *Living Reviews in Solar Physics*, *11*, 3, doi:10.12942/lrsp-2014-3, 2014.

Cheung, M. C. M., et al., Homologous Helical Jets: Observations By IRIS, SDO, and Hinode and Magnetic Modeling With Data-Driven Simulations, *Astrophys. J.*, *801*, 83, doi:10.1088/0004-637X/801/2/83, 2015.

Cohen, O., et al., A Semiempirical Magnetohydrodynamical Model of the Solar Wind, *Astrophys. J.,* , *654*, L163–L166, doi:10.1086/511154, 2007.

Cremades, H., and V. Bothmer, On the three-dimensional configuration of coronal mass ejections, *Astronom. Astrophys.*, *422*, 307–322, doi:10.1051/0004-6361:20035776, 2004.

Cyr, O. C. S., M. A. Mesarch, H. M. Maldonado, D. C. Folta, A. D. Harper, J. M. Davila, and R. R. Fisher, Space Weather Diamond: a four spacecraft monitoring system, *Journal of Atmospheric and Solar-Terrestrial Physics*, *62*, 1251–1255, doi:10.1016/S1364-6826(00)00069-9, 2000.

Daldorff, L. K. S., G. Tóth, T. I. Gombosi, G. Lapenta, J. Amaya, S. Markidis, and

©2019 American Geophysical Union. All Rights Reserved.

Accepted Article

J. U. Brackbill, Two-way coupling of a global Hall magnetohydrodynamics model with a local implicit particle-in-cell model, *Journal of Computational Physics*, *268*, 236–254, doi:10.1016/j.jcp.2014.03.009, 2014.

Dasso, S., M. S. Nakwacki, P. Démoulin, and C. H. Mandrini, Progressive Transformation of a Flux Rope to an ICME. Comparative Analysis Using the Direct and Fitted Expansion Methods, *Sol. Phys.*, *244*, 115–137, doi:10.1007/s11207-007-9034-2, 2007.

Davis, C. J., J. A. Davies, M. Lockwood, A. P. Rouillard, C. J. Eyles, and R. A. Harrison, Stereoscopic imaging of an Earth-impacting solar coronal mass ejection: A major milestone for the STEREO mission, *Geophys. Res. Lett.*, *36*, L08102, doi:10.1029/2009GL038021, 2009.

Desai, M., and J. Giacalone, Large gradual solar energetic particle events, *Living Reviews in Solar Physics*, *13*, 3, doi:10.1007/s41116-016-0002-5, 2016.

D'Huys, E., D. B. Seaton, S. Poedts, and D. Berghmans, Observational Characteristics of Coronal Mass Ejections without Low-coronal Signatures, *Astrophys. J.*, *795*, 49, doi:10.1088/0004-637X/795/1/49, 2014.

Dissauer, K., A. M. Veronig, M. Temmer, and T. Podladchikova, Statistics of coronal dimmings associated with coronal mass ejections. II. Relationship between coronal dimmings and their associated CMEs, *ArXiv e-prints*, 2018.

Dryer, M., Interplanetary Shock Waves Generated by Solar Flares, *Space Sci. Rev.*, *15*, 403–468, doi:10.1007/BF00178215, 1974.

Dungey, J. W., Interplanetary Magnetic Field and the Auroral Zones, *Physical Review Letters*, *6*, 47–48, doi:10.1103/PhysRevLett.6.47, 1961.

Eastwood, E. H. M. A. G. L. B. M. M. B. R. D. W. R. M. L. G. M. B. C., J. P. Biffis, The

©2019 American Geophysical Union. All Rights Reserved.

Accepted Article

Economic Impact of Space Weather: Where Do We Stand?, *Risk Analysis*, *37*, 206–28, doi:10.1111/risa.12765, 2017.

Eastwood, E. H. M. A. G. L. B. M. M. B. R. D. W. R. M. L. G. M. B. C., J. P. Biffis, Quantifying the Economic Value of Space Weather Forecasting for Power Grids: An Exploratory Study, *Risk Analysis*, 2018.

Eyles, C. J., et al., The Heliospheric Imagers Onboard the STEREO Mission, *Sol. Phys.*, *254*, 387–445, doi:10.1007/s11207-008-9299-0, 2009.

Fan, Y., The Emergence of a Twisted Ω-Tube into the Solar Atmosphere, *Astrophys. J.*, *554*, L111–L114, doi:10.1086/320935, 2001.

Fan, Y., S. Gibson, and S. Tomczyk, The eruption of a prominence carrying coronal flux rope: forward synthesis of the magnetic field strength measurement by the COronal Solar Magnetism Observatory Large Coronagraph, *ArXiv e-prints*, 2018.

Fang, F., W. Manchester, W. P. Abbett, and B. van der Holst, Simulation of Flux Emergence from the Convection Zone to the Corona, *Astrophys. J.,* , *714*, 1649–1657, doi:10.1088/0004-637X/714/2/1649, 2010.

Farrugia, C. J., V. K. Jordanova, M. F. Thomsen, G. Lu, S. W. H. Cowley, and K. W. Ogilvie, A two-ejecta event associated with a two-step geomagnetic storm, *Journal of Geophysical Research (Space Physics)*, *111*, A11104, doi:10.1029/2006JA011893, 2006.

Farrugia, C. J., et al., Multiple, distant (40 deg) in situ observations of a magnetic cloud and a corotating interaction region complex, *Journal of Atmospheric and Solar-Terrestrial Physics*, *73*, 1254–1269, doi:10.1016/j.jastp.2010.09.011, 2011.

Fisher, G. H., B. T. Welsch, W. P. Abbett, and D. J. Bercik, Estimating Electric Fields from Vector Magnetogram Sequences, *Astrophys. J.*, *715*, 242–259, doi:

Accepted Article

©2019 American Geophysical Union. All Rights Reserved.

10.1088/0004-637X/715/1/242, 2010.

Fisher, G. H., et al., The Coronal Global Evolutionary Model: Using HMI Vector Magnetogram and Doppler Data to Model the Buildup of Free Magnetic Energy in the Solar Corona, *Space Weather*, *13*, 369–373, doi:10.1002/2015SW001191, 2015.

Forbes, T. G., A review on the genesis of coronal mass ejections, *J. Geophys. Res.*, *105*, 23,153–23,166, doi:10.1029/2000JA000005, 2000.

Ganushkina, N. Y., O. A. Amariutei, D. Welling, and D. Heynderickx, Nowcast model for low-energy electrons in the inner magnetosphere, *Space Weather*, *13*, 16–34, doi:10.1002/2014SW001098, 2015.

Gibney, E., Space-weather forecast to improve with European satellite, *Nature*, *541*, 271, doi:10.1038/541271a, 2017.

Gibson, S. E., and B. C. Low, Three-dimensional and twisted: An MHD interpretation of on-disk observational characteristics of coronal mass ejections, *J. Geophys. Res.*, *105*, 18,187–18,202, doi:10.1029/1999JA000317, 2000.

Gonzalez, W. D., J. A. Joselyn, Y. Kamide, H. W. Kroehl, G. Rostoker, B. T. Tsurutani, and V. M. Vasyliunas, What is a geomagnetic storm?, *J. Geophys. Res.*, *99*, 5771–5792, doi:10.1029/93JA02867, 1994.

Good, S. W., and R. J. Forsyth, Interplanetary Coronal Mass Ejections Observed by MESSENGER and Venus Express, *Sol. Phys*, *291*, 239–263, doi:10.1007/s11207-015-0828-3, 2016.

Gopalswamy, N., A. Lara, S. Yashiro, M. L. Kaiser, and R. A. Howard, Predicting the 1-AU arrival times of coronal mass ejections, *J. Geophys. Res.*, *106*, 29,207–29,218, doi:10.1029/2001JA000177, 2001a.

©2019 American Geophysical Union. All Rights Reserved.

Accepted Article

Gopalswamy, N., S. Yashiro, M. L. Kaiser, R. A. Howard, and J.-L. Bougeret, Radio Signatures of Coronal Mass Ejection Interaction: Coronal Mass Ejection Cannibalism?, *Astrophys. J. Lett.*, *548*, L91–L94, doi:10.1086/318939, 2001b.

Gopalswamy, N., S. Yashiro, S. Akiyama, and H. Xie, Estimation of Reconnection Flux Using Post-eruption Arcades and Its Relevance to Magnetic Clouds at 1 AU, *Sol. Phys.*, *292*, 65, doi:10.1007/s11207-017-1080-9, 2017.

Gopalswamy, N., S. Akiyama, S. Yashiro, and H. Xie, A New Technique to Provide Realistic Input to CME Forecasting Models, in *Space Weather of the Heliosphere: Processes and Forecasts*, *IAU Symposium*, vol. 335, edited by C. Foullon and O. E. Malandraki, pp. 258–262, doi:10.1017/S1743921317011048, 2018.

Gosling, J. T., Coronal mass ejections and magnetic flux ropes in interplanetary space, *Washington DC American Geophysical Union Geophysical Monograph Series*, *58*, 343–364, doi:10.1029/GM058p0343, 1990.

Gosling, J. T., D. N. Baker, S. J. Bame, W. C. Feldman, R. D. Zwickl, and E. J. Smith, Bidirectional solar wind electron heat flux events, *J. Geophys. Res.*, *92*, 8519–8535, doi:10.1029/JA092iA08p08519, 1987.

Gosling, J. T., D. J. McComas, J. L. Phillips, and S. J. Bame, Geomagnetic activity associated with earth passage of interplanetary shock disturbances and coronal mass ejections, *J. Geophys. Res.*, *96*, 7831–7839, doi:10.1029/91JA00316, 1991.

Green, L. M., and B. Kliem, Flux Rope Formation Preceding Coronal Mass Ejection Onset, *Astrophys. J. Lett.*, *700*, L83–L87, doi:10.1088/0004-637X/700/2/L83, 2009.

Green, L. M., B. Kliem, and A. J. Wallace, Photospheric flux cancellation and associated flux rope formation and eruption, *Astron. Astrophys.*, *526*, A2, doi:10.1051/0004-6361/

Accepted Article

©2019 American Geophysical Union. All Rights Reserved.

201015146, 2011.

Green, L. M., T. Török, B. Vršnak, W. Manchester, and A. Veronig, The Origin, Early Evolution and Predictability of Solar Eruptions, *Space Sci. Rev.*, *214*, 46, doi:10.1007/s11214-017-0462-5, 2018.

Gulisano, A. M., P. Démoulin, S. Dasso, M. E. Ruiz, and E. Marsch, Global and local expansion of magnetic clouds in the inner heliosphere, *Astron. and Astrophys.*, *509*, A39, doi:10.1051/0004-6361/200912375, 2010.

Guo, J., F. Wei, X. Feng, J. M. Forbes, Y. Wang, H. Liu, W. Wan, Z. Yang, and C. Liu, Prolonged multiple excitation of large-scale Traveling Atmospheric Disturbances (TADs) by successive and interacting coronal mass ejections, *J. Geophys. Res.*, *121*, 2662–2668, doi:10.1002/2015JA022076, 2016.

Harrison, R. A., C. J. Davis, and C. J. Eyles, The STEREO heliospheric imager: how to detect CMEs in the heliosphere, *Advances in Space Research*, *36*, 1512–1523, doi:10.1016/j.asr.2005.01.024, 2005.

Harrison, R. A., et al., CMEs in the Heliosphere: I. A Statistical Analysis of the Observational Properties of CMEs Detected in the Heliosphere from 2007 to 2017 by STEREO/HI-1, *Sol. Phys.*, *293*, 77, doi:10.1007/s11207-018-1297-2, 2018.

Henney, C. J., W. A. Toussaint, S. M. White, and C. N. Arge, Forecasting $F_{10.7}$ with solar magnetic flux transport modeling, *Space Weather*, *10*, S02011, doi:10.1029/2011SW000748, 2012.

Howard, R. A., D. J. Michels, N. R. Sheeley, Jr., and M. J. Koomen, The observation of a coronal transient directed at earth, *Astrop. J. Lett.*, *263*, L101–L104, doi:10.1086/183932, 1982.

©2019 American Geophysical Union. All Rights Reserved.

Accepted Article

Howard, R. A., et al., Sun Earth Connection Coronal and Heliospheric Investigation (SECCHI), *Space Sci. Rev.*, *136*, 67–115, doi:10.1007/s11214-008-9341-4, 2008a.

Howard, T. A., and C. E. DeForest, The Thomson Surface. I. Reality and Myth, *Astrophys. J.*, *752*, 130, doi:10.1088/0004-637X/752/2/130, 2012.

Howard, T. A., D. Nandy, and A. C. Koepke, Kinematic properties of solar coronal mass ejections: Correction for projection effects in spacecraft coronagraph measurements, *Journal of Geophysical Research (Space Physics)*, *113*, A01104, doi:10.1029/2007JA012500, 2008b.

Howard, T. A., K. Stovall, J. Dowell, G. B. Taylor, and S. M. White, Measuring the Magnetic Field of Coronal Mass Ejections Near the Sun Using Pulsars, *Astrophys. J.*, *831*, 208, doi:10.3847/0004-637X/831/2/208, 2016.

Hu, Q., J. Qiu, B. Dasgupta, A. Khare, and G. M. Webb, Structures of Interplanetary Magnetic Flux Ropes and Comparison with Their Solar Sources, *Astrophys. J.*, *793*, 53, doi:10.1088/0004-637X/793/1/53, 2014.

Hundhausen, A. J., Sizes and locations of coronal mass ejections - SMM observations from 1980 and 1984-1989, *J. Geophys. Res.*, *98*, 13, doi:10.1029/93JA00157, 1993.

Hundhausen, A. J., C. B. Sawyer, L. House, R. M. E. Illing, and W. J. Wagner, Coronal mass ejections observed during the solar maximum mission: Latitude distribution and rate of occurrence, *J. Geophys. Res.*, *89*, 2639–2646, doi:10.1029/JA089iA05p02639, 1984.

Huttunen, K. E. J., H. E. J. Koskinen, T. I. Pulkkinen, A. Pulkkinen, M. Palmroth, E. G. D. Reeves, and H. J. Singer, April 2000 magnetic storm: Solar wind driver and magnetospheric response, *Journal of Geophysical Research (Space Physics)*, *107*, 1440,

©2019 American Geophysical Union. All Rights Reserved.

Accepted Article

doi:10.1029/2001JA009154, 2002.

Huttunen, K. E. J., R. Schwenn, V. Bothmer, and H. E. J. Koskinen, Properties and geoeffectiveness of magnetic clouds in the rising, maximum and early declining phases of solar cycle 23, *Annales Geophysicae*, *23*, 625–641, doi:10.5194/angeo-23-625-2005, 2005.

Illing, R. M. E., and A. J. Hundhausen, Observation of a coronal transient from 1.2 to 6 solar radii, *J. Geophys. Res*, *90*, 275–282, doi:10.1029/JA090iA01p00275, 1985.

Isavnin, A., FRiED: A Novel Three-dimensional Model of Coronal Mass Ejections, *Astrophys. J.*, *833*, 267, doi:10.3847/1538-4357/833/2/267, 2016.

Isavnin, A., A. Vourlidas, and E. K. J. Kilpua, Three-Dimensional Evolution of Flux-Rope CMEs and Its Relation to the Local Orientation of the Heliospheric Current Sheet, *Sol. Phys.*, *289*, 2141–2156, doi:10.1007/s11207-013-0468-4, 2014.

Jackson, B., P. Hick, A. Buffington, H.-S. Yu, and G. Zhao, Bz Determinations and Forecasts Using UCSD Analysis Techniques, in *42nd COSPAR Scientific Assembly*, *COSPAR Meeting*, vol. 42, pp. D2.3–22–18, 2018.

James, A. W., L. M. Green, E. Palmerio, G. Valori, H. A. S. Reid, D. Baker, D. H. Brooks, L. van Driel-Gesztelyi, and E. K. J. Kilpua, On-Disc Observations of Flux Rope Formation Prior to Its Eruption, *Sol. Phys.*, *292*, 71, doi:10.1007/s11207-017-1093-4, 2017.

Jang, S., Y.-J. Moon, R.-S. Kim, H. Lee, and K.-S. Cho, Comparison between 2D and 3D Parameters of 306 Front-side Halo CMEs from 2009 to 2013, *Astrophys. J.*, *821*, 95, doi:10.3847/0004-637X/821/2/95, 2016.

Janvier, M., P. Démoulin, and S. Dasso, Global axis shape of magnetic clouds deduced

Accepted Article

©2019 American Geophysical Union. All Rights Reserved.

from the distribution of their local axis orientation, *Astrophys and Astron.*, *556*, A50, doi:10.1051/0004-6361/201321442, 2013.

Jian, L., C. T. Russell, J. G. Luhmann, and R. M. Skoug, Properties of Interplanetary Coronal Mass Ejections at One AU During 1995–2004, *Sol. Phys.*, *239*, 393–436, doi:10.1007/s11207-006-0133-2, 2006.

Jiang, C., S. T. Wu, X. Feng, and Q. Hu, Data-driven magnetohydrodynamic modelling of a flux-emerging active region leading to solar eruption, *Nature Communications*, *7*, 11522, doi:10.1038/ncomms11522, 2016.

Jin, M., C. J. Schrijver, M. C. M. Cheung, M. L. DeRosa, N. V. Nitta, and A. M. Title, A Numerical Study of Long-range Magnetic Impacts during Coronal Mass Ejections, *Astrophys. J.*, *820*, 16, doi:10.3847/0004-637X/820/1/16, 2016.

Jin, M., W. B. Manchester, B. van der Holst, I. Sokolov, G. Tóth, R. E. Mullinix, A. Taktakishvili, A. Chulaki, and T. I. Gombosi, Data-constrained Coronal Mass Ejections in a Global Magnetohydrodynamics Model, *Astrophys. J.*, *834*, 173, doi:10.3847/1538-4357/834/2/173, 2017.

Kataoka, R., D. Shiota, E. Kilpua, and K. Keika, Pileup accident hypothesis of magnetic storm on 17 March 2015, *Geophys. Res. Lett.*, *42*, 5155–5161, doi:10.1002/2015GL064816, 2015.

Kay, C., and N. Gopalswamy, Using the Coronal Evolution to Successfully Forward Model CMEs' In Situ Magnetic Profiles, *Journal of Geophysical Research (Space Physics)*, *122*, 11, doi:10.1002/2017JA024541, 2017.

Kay, C., and M. Opher, The Heliocentric Distance where the Deflections and Rotations of Solar Coronal Mass Ejections Occur, *Astrophys. J. Lett.*, *811*, L36, doi:10.1088/

Accepted Article

©2019 American Geophysical Union. All Rights Reserved.

2041-8205/811/2/L36, 2015.

Kay, C., M. Opher, and R. M. Evans, Forecasting a Coronal Mass Ejection's Altered Trajectory: ForeCAT, *Astrophys. J.*, *775*, 5, doi:10.1088/0004-637X/775/1/5, 2013.

Kay, C., N. Gopalswamy, A. Reinard, and M. Opher, Predicting the Magnetic Field of Earth-impacting CMEs, *Astrophys. J.*, *835*, 117, doi:10.3847/1538-4357/835/2/117, 2017.

Kazachenko, M. D., G. H. Fisher, and B. T. Welsch, A Comprehensive Method of Estimating Electric Fields from Vector Magnetic Field and Doppler Measurements, *Astrophys. J.*, *795*, 17, doi:10.1088/0004-637X/795/1/17, 2014.

Kilpua, E., H. E. J. Koskinen, and T. I. Pulkkinen, Coronal mass ejections and their sheath regions in interplanetary space, *Living Reviews in Solar Physics*, *14*, 5, doi:10.1007/s41116-017-0009-6, 2017.

Kilpua, E. K. J., L. K. Jian, Y. Li, J. G. Luhmann, and C. T. Russell, Multipoint ICME encounters: Pre-STEREO and STEREO observations, *J. Atmos. Terr. Phys.*, *73*, 1228–1241, doi:10.1016/j.jastp.2010.10.012, 2011.

Kilpua, E. K. J., A. Isavnin, A. Vourlidas, H. E. J. Koskinen, and L. Rodriguez, On the relationship between interplanetary coronal mass ejections and magnetic clouds, *Annales Geophysicae*, *31*, 1251–1265, doi:10.5194/angeo-31-1251-2013, 2013.

Kilpua, E. K. J., M. Mierla, A. N. Zhukov, L. Rodriguez, A. Vourlidas, and B. Wood, Solar Sources of Interplanetary Coronal Mass Ejections During the Solar Cycle 23/24 Minimum, *Sol. Phys.*, *289*, 3773–3797, doi:10.1007/s11207-014-0552-4, 2014.

Klein, L. W., and L. F. Burlaga, Interplanetary magnetic clouds at 1 AU, *J. Geophys. Res.*, *87*, 613–624, doi:10.1029/JA087iA02p00613, 1982.

©2019 American Geophysical Union. All Rights Reserved.

Accepted Article

Kliem, B., and T. Török, Torus Instability, *Physical Review Letters*, *96*(25), 255002, doi:10.1103/PhysRevLett.96.255002, 2006.

Kliem, B., T. G. Forbes, S. Patsourakos, and A. Vourlidas, Rapid CME Cavity Formation and Expansion, in *American Astronomical Society Meeting Abstracts #224*, *American Astronomical Society Meeting Abstracts*, vol. 224, p. 212.06, 2014.

Kooi, J. E., P. D. Fischer, J. J. Buffo, and S. R. Spangler, VLA Measurements of Faraday Rotation through Coronal Mass Ejections, *Sol. Phys.*, *292*, 56, doi:10.1007/s11207-017-1074-7, 2017.

Krauss, S., M. Temmer, A. Veronig, O. Baur, and H. Lammer, Thermospheric and geomagnetic responses to interplanetary coronal mass ejections observed by ACE and GRACE: Statistical results, *Journal of Geophysical Research (Space Physics)*, *120*, 8848–8860, doi:10.1002/2015JA021702, 2015.

Kubicka, M., C. Möstl, T. Amerstorfer, P. D. Boakes, L. Feng, J. P. Eastwood, and O. Törmänen, Prediction of Geomagnetic Storm Strength from Inner Heliospheric In Situ Observations, *Astrophys. J.*, *833*, 255, doi:10.3847/1538-4357/833/2/255, 2016.

Kwon, R.-Y., J. Zhang, and A. Vourlidas, Are Halo-like Solar Coronal Mass Ejections Merely a Matter of Geometric Projection Effects?, *ApJ Letters*, *799*, L29, doi:10.1088/2041-8205/799/2/L29, 2015.

Lagg, A., B. Lites, J. Harvey, S. Gosain, and R. Centeno, Measurements of Photospheric and Chromospheric Magnetic Fields, *Space Sci. Rev.*, *210*, 37–76, doi:10.1007/s11214-015-0219-y, 2017.

Lara, A., N. Gopalswamy, H. Xie, E. Mendoza-Torres, R. PéRez-EríQuez, and G. Michalek, Are halo coronal mass ejections special events?, *Journal of Geophysical*

Accepted Article

©2019 American Geophysical Union. All Rights Reserved.

Research (Space Physics), *111*, A06107, doi:10.1029/2005JA011431, 2006.

Lavraud, B., et al., A small mission concept to the Sun-Earth Lagrangian L5 point for innovative solar, heliospheric and space weather science, *Journal of Atmospheric and Solar-Terrestrial Physics*, *146*, 171–185, doi:10.1016/j.jastp.2016.06.004, 2016.

Lee, C. O., C. N. Arge, D. Odstrčil, G. Millward, V. Pizzo, J. M. Quinn, and C. J. Henney, Ensemble Modeling of CME Propagation, *Sol. Phys.*, *285*, 349–368, doi:10.1007/s11207-012-9980-1, 2013.

Lee, H., Y.-J. Moon, H. Na, S. Jang, and J.-O. Lee, Are 3-D coronal mass ejection parameters from single-view observations consistent with multiview ones?, *Journal of Geophysical Research (Space Physics)*, *120*, 10, doi:10.1002/2015JA021118, 2015.

Leitner, M., C. J. Farrugia, C. MöStl, K. W. Ogilvie, A. B. Galvin, R. Schwenn, and H. K. Biernat, Consequences of the force-free model of magnetic clouds for their heliospheric evolution, *Journal of Geophysical Research (Space Physics)*, *112*, A06113, doi:10.1029/2006JA011940, 2007.

Lin, H., J. R. Kuhn, and R. Coulter, Coronal Magnetic Field Measurements, *Astrophys. J. Lett.*, *613*, L177–L180, doi:10.1086/425217, 2004.

Lindsay, G. M., C. T. Russell, and J. G. Luhmann, Predictability of Dst index based upon solar wind conditions monitored inside 1 AU, *J. Geophys. Res.*, *104*, 10,335–10,344, doi:10.1029/1999JA900010, 1999.

Liu, Y., W. B. Manchester, IV, J. C. Kasper, J. D. Richardson, and J. W. Belcher, Determining the Magnetic Field Orientation of Coronal Mass Ejections from Faraday Rotation, *Astrophys. J.*, *665*, 1439–1447, doi:10.1086/520038, 2007.

Liu, Y. D., et al., Interactions between Coronal Mass Ejections Viewed in Coordinated

©2019 American Geophysical Union. All Rights Reserved.

Accepted Article

Imaging and in situ Observations, *ApJ Letters*, *746*, L15, doi:10.1088/2041-8205/746/2/L15, 2012.

Liu, Y. D., et al., Observations of an extreme storm in interplanetary space caused by successive coronal mass ejections, *Nature Communications*, *5*, 3481, doi:10.1038/ncomms4481, 2014.

Long, D. M., L. K. Harra, S. A. Matthews, H. P. Warren, K.-S. Lee, G. A. Doschek, H. Hara, and J. M. Jenkins, Plasma Evolution within an Erupting Coronal Cavity, *Astrophys. J.*, *855*, 74, doi:10.3847/1538-4357/aaad68, 2018.

Longcope, D., C. Beveridge, J. Qiu, B. Ravindra, G. Barnes, and S. Dasso, Modeling and Measuring the Flux Reconnected and Ejected by the Two-Ribbon Flare/CME Event on 7 November 2004, *Sol. Phys.*, *244*, 45–73, doi:10.1007/s11207-007-0330-7, 2007.

Lugaz, N., W. B. Manchester, IV, and T. I. Gombosi, Numerical Simulation of the Interaction of Two Coronal Mass Ejections from Sun to Earth, *Astrophys. J.,* , *634*, 651–662, doi:10.1086/491782, 2005.

Lugaz, N., W. B. Manchester, IV, I. I. Roussev, G. Tóth, and T. I. Gombosi, Numerical Investigation of the Homologous Coronal Mass Ejection Events from Active Region 9236, *Astrophys. J.*, *659*, 788–800, doi:10.1086/512005, 2007.

Lugaz, N., C. J. Farrugia, W. B. Manchester, IV, and N. Schwadron, The Interaction of Two Coronal Mass Ejections: Influence of Relative Orientation, *Astrophys. J.*, *778*, 20, doi:10.1088/0004-637X/778/1/20, 2013.

Lugaz, N., C. J. Farrugia, C.-L. Huang, and H. E. Spence, Extreme geomagnetic disturbances due to shocks within CMEs, *Geophys. Res. Lett.*, *42*, 4694–4701, doi:10.1002/2015GL064530, 2015a.

©2019 American Geophysical Union. All Rights Reserved.

Accepted Article

Lugaz, N., C. J. Farrugia, C. W. Smith, and K. Paulson, Shocks inside CMEs: A survey of properties from 1997 to 2006, *Journal of Geophysical Research (Space Physics)*, *120*, 2409–2427, doi:10.1002/2014JA020848, 2015b.

Lugaz, N., M. Temmer, Y. Wang, and C. J. Farrugia, The Interaction of Successive Coronal Mass Ejections: A Review, *Solar Phys.*, *292*, 64, doi:10.1007/s11207-017-1091-6, 2017.

Lugaz, N., C. J. Farrugia, R. M. Winslow, N. Al-Haddad, A. B. Galvin, T. Nieves-Chinchilla, C. O. Lee, and M. Janvier, On the Spatial Coherence of Magnetic Ejecta: Measurements of Coronal Mass Ejections by Multiple Spacecraft Longitudinally Separated by 0.01 au, *Astrophys. J. Lett.*, *864*, L7, doi:10.3847/2041-8213/aad9f4, 2018.

Lumme, E., J. Pomoell, and E. K. J. Kilpua, Optimization of Photospheric Electric Field Estimates for Accurate Retrieval of Total Magnetic Energy Injection, *Sol. Phys.*, *292*, 191, doi:10.1007/s11207-017-1214-0, 2017.

Lundquist, S., On the Stability of Magneto-Hydrostatic Fields, *Physical Review*, *83*, 307–311, doi:10.1103/PhysRev.83.307, 1951.

Lynch, B. J., S. K. Antiochos, P. J. MacNeice, T. H. Zurbuchen, and L. A. Fisk, Observable Properties of the Breakout Model for Coronal Mass Ejections, *Astrophys. J.*, *617*, 589–599, doi:10.1086/424564, 2004.

Lynch, B. J., S. K. Antiochos, Y. Li, J. G. Luhmann, and C. R. DeVore, Rotation of Coronal Mass Ejections during Eruption, *Astrophys. J.*, *697*, 1918–1927, doi:10.1088/0004-637X/697/2/1918, 2009.

Mackay, D. H., A. R. Yeates, and F.-X. Bocquet, Impact of an L5 Magnetograph on Nonpotential Solar Global Magnetic Field Modeling, *Astrophys. J.*, *825*, 131, doi:10.

©2019 American Geophysical Union. All Rights Reserved.

Accepted Article

3847/0004-637X/825/2/131, 2016.

Makwana, K. D., R. Keppens, and G. Lapenta, Study of magnetic reconnection in large-scale magnetic island coalescence via spatially coupled MHD and PIC simulations, *Physics of Plasmas*, *25*(8), 082904, doi:10.1063/1.5037774, 2018.

Manchester, W., E. K. J. Kilpua, Y. D. Liu, N. Lugaz, P. Riley, T. Török, and B. Vršnak, The Physical Processes of CME/ICME Evolution, *Space Sci. Rev.*, *212*, 1159–1219, doi:10.1007/s11214-017-0394-0, 2017.

Manchester, W. B., T. I. Gombosi, I. Roussev, A. Ridley, D. L. de Zeeuw, I. V. Sokolov, K. G. Powell, and G. Tóth, Modeling a space weather event from the Sun to the Earth: CME generation and interplanetary propagation, *Journal of Geophysical Research (Space Physics)*, *109*, A02107, doi:10.1029/2003JA010150, 2004.

Mandrini, C. H., S. Pohjolainen, S. Dasso, L. M. Green, P. Démoulin, L. van Driel-Gesztelyi, C. Copperwheat, and C. Foley, Interplanetary flux rope ejected from an X-ray bright point. The smallest magnetic cloud source-region ever observed, *Astron. Astrophys.*, *434*, 725–740, doi:10.1051/0004-6361:20041079, 2005.

Martens, P. C., and C. Zwaan, Origin and Evolution of Filament-Prominence Systems, *Astrophys. J.*, *558*, 872–887, doi:10.1086/322279, 2001.

Martínez-Sykora, J., V. Hansteen, and M. Carlsson, Twisted Flux Tube Emergence From the Convection Zone to the Corona, *Astrophys. J.*, *679*, 871–888, doi:10.1086/587028, 2008.

Mayaud, P., *Derivation, Meaning, and Use of Geomagnetic Indices*, *Geophysical Monograph*, vol. 22, American Geophysical Union, Washington, DC, 1980.

Accepted Article

©2019 American Geophysical Union. All Rights Reserved.

Mays, M. L., et al., Propagation of the 7 January 2014 CME and Resulting Geomagnetic Non-event, *Astrophys. J.*, *812*, 145, doi:10.1088/0004-637X/812/2/145, 2015a.

Mays, M. L., et al., Ensemble Modeling of CMEs Using the WSA-ENLIL+Cone Model, *Solar Phys.*, *290*, 1775–1814, doi:10.1007/s11207-015-0692-1, 2015b.

Mendillo, M., and C. Narvaez, Ionospheric storms at geophysically-equivalent sites - Part 1: Storm-time patterns for sub-auroral ionospheres, *Annales Geophysicae*, *27*, 1679–1694, doi:10.5194/angeo-27-1679-2009, 2009.

Mendillo, M., and C. Narvaez, Ionospheric storms at geophysically-equivalent sites - Part 2: Local time storm patterns for sub-auroral ionospheres, *Annales Geophysicae*, *28*, 1449–1462, doi:10.5194/angeo-28-1449-2010, 2010.

Michałek, G., N. Gopalswamy, and S. Yashiro, A New Method for Estimating Widths, Velocities, and Source Location of Halo Coronal Mass Ejections, *Astrophys. J.*, *584*, 472–478, doi:10.1086/345526, 2003.

Mierla, M., et al., On the 3-D reconstruction of Coronal Mass Ejections using coronagraph data, *Annales Geophysicae*, *28*, 203–215, doi:10.5194/angeo-28-203-2010, 2010.

Mikic, Z., and J. A. Linker, Large-scale structure of the solar corona and inner heliosphere, in *Solar Wind Eight*, p. 60, 1995.

Mikić, Z., J. A. Linker, D. D. Schnack, R. Lionello, and A. Tarditi, Magnetohydrodynamic modeling of the global solar corona, *Physics of Plasmas*, *6*, 2217–2224, doi:10.1063/1.873474, 1999.

Millward, G., D. Biesecker, V. Pizzo, and C. A. de Koning, An operational software tool for the analysis of coronagraph images: Determining CME parameters for input into the WSA-Enlil heliospheric model, *Space Weather*, *11*, 57–68, doi:10.1002/swe.20024,

Accepted Article

©2019 American Geophysical Union. All Rights Reserved.

2013.

Mishra, W., N. Srivastava, and T. Singh, Kinematics of interacting CMEs of 25 and 28 September 2012, *Journal of Geophysical Research (Space Physics)*, *120*, 10, doi: 10.1002/2015JA021415, 2015.

Möstl, C., C. J. Farrugia, M. Temmer, C. Miklenic, A. M. Veronig, A. B. Galvin, M. Leitner, and H. K. Biernat, Linking Remote Imagery of a Coronal Mass Ejection to Its In Situ Signatures at 1 AU, *Astrophys. J. Letters*, *705*, L180–L185, doi: 10.1088/0004-637X/705/2/L180, 2009.

Möstl, C., et al., Multi-point Shock and Flux Rope Analysis of Multiple Interplanetary Coronal Mass Ejections around 2010 August 1 in the Inner Heliosphere, *Astrophys. J.*, *758*, 10, doi:10.1088/0004-637X/758/1/10, 2012.

Möstl, C., et al., Strong coronal channelling and interplanetary evolution of a solar storm up to Earth and Mars, *Nature Communications*, *6*, 7135, doi:10.1038/ncomms8135, 2015.

Möstl, C., et al., Modeling observations of solar coronal mass ejections with heliospheric imagers verified with the Heliophysics System Observatory, *Space Weather*, *15*, 955–970, doi:10.1002/2017SW001614, 2017.

Möstl, C., et al., Forward Modeling of Coronal Mass Ejection Flux Ropes in the Inner Heliosphere with 3DCORE, *Space Weather*, *16*, 216–229, doi:10.1002/2017SW001735, 2018.

Müller, D., R. G. Marsden, O. C. St. Cyr, and H. R. Gilbert, Solar Orbiter . Exploring the Sun-Heliosphere Connection, *Solar Phys.*, *285*, 25–70, doi:10.1007/s11207-012-0085-7, 2013.

Accepted Article

©2019 American Geophysical Union. All Rights Reserved.

Mulligan, T., C. T. Russell, and J. G. Luhmann, Solar cycle evolution of the structure of magnetic clouds in the inner heliosphere, *Geophys. Res. Lett.*, *25*, 2959–2962, doi: 10.1029/98GL01302, 1998.

Munro, R. H., J. T. Gosling, E. Hildner, R. M. MacQueen, A. I. Poland, and C. L. Ross, The association of coronal mass ejection transients with other forms of solar activity, *Sol. Phys.*, *61*, 201–215, doi:10.1007/BF00155456, 1979.

Ngwira, C. M., et al., Simulation of the 23 July 2012 extreme space weather event: What if this extremely rare CME was Earth directed?, *Space Weather*, *11*, 671–679, doi: 10.1002/2013SW000990, 2013.

Nitta, N. V., and T. Mulligan, Earth-Affecting Coronal Mass Ejections Without Obvious Low Coronal Signatures, *Sol. Phys.*, *292*, 125, doi:10.1007/s11207-017-1147-7, 2017.

Odstrcil, D., Operational simulation of heliospheric space weather: Improvements of the WSA-ENLIL-Cone modeling system, in *42nd COSPAR Scientific Assembly*, *COSPAR Meeting*, vol. 42, pp. D2.3–42–18, 2018.

Odstrcil, D., J. A. Linker, R. Lionello, Z. Mikic, P. Riley, V. J. Pizzo, and J. G. Luhmann, Merging of coronal and heliospheric numerical two-dimensional MHD models, *Journal of Geophysical Research (Space Physics)*, *107*, 1493, doi:10.1029/2002JA009334, 2002.

Odstrcil, D., N. Savani, and A. Rouillard, Launching CME-like Disturbances into the Operational Heliospheric Space Weather Models, in *Solar Heliospheric and INterplanetary Environment (SHINE 2018)*, p. 123, 2018.

Odstrčil, D., and V. J. Pizzo, Three-dimensional propagation of CMEs in a structured solar wind flow: 1. CME launched within the streamer belt, *J. Geophys. Res.*, *104*, 483–492, doi:10.1029/1998JA900019, 1999.

©2019 American Geophysical Union. All Rights Reserved.

Accepted Article

Owens, M., and P. Cargill, Predictions of the arrival time of Coronal Mass Ejections at 1AU: an analysis of the causes of errors, *Annales Geophysicae*, *22*, 661–671, doi:10.5194/angeo-22-661-2004, 2004.

Owens, M. J., M. Lockwood, and L. A. Barnard, Coronal mass ejections are not coherent magnetohydrodynamic structures, *Scientific Reports*, *7*, 4152, doi:10.1038/s41598-017-04546-3, 2017a.

Owens, M. J., P. Riley, and T. S. Horbury, Probabilistic Solar Wind and Geomagnetic Forecasting Using an Analogue Ensemble or "Similar Day" Approach, *Solar Phys.*, *292*, 69, doi:10.1007/s11207-017-1090-7, 2017b.

Pagano, P., D. H. Mackay, and A. R. Yeates, A new technique for observationally derived boundary conditions for space weather, *Journal of Space Weather and Space Climate*, *8*(27), A26, doi:10.1051/swsc/2018012, 2018.

Palmerio, E., E. K. J. Kilpua, A. W. James, L. M. Green, J. Pomoell, A. Isavnin, and G. Valori, Determining the Intrinsic CME Flux Rope Type Using Remote-sensing Solar Disk Observations, *Solar Phys.*, *292*, 39, doi:10.1007/s11207-017-1063-x, 2017.

Palmerio, E., E. K. J. Kilpua, C. Möstl, V. Bothmer, A. W. James, L. M. Green, A. Isavnin, J. A. Davies, and R. A. Harrison, Coronal Magnetic Structure of Earthbound CMEs and In Situ Comparison, *Space Weather*, *16*, 442–460, doi:10.1002/2017SW001767, 2018.

Panasenco, O., S. F. Martin, M. Velli, and A. Vourlidas, Origins of Rolling, Twisting, and Non-radial Propagation of Eruptive Solar Events, *Solar Phys.*, *287*, 391–413, doi:10.1007/s11207-012-0194-3, 2013.

Accepted Article

©2019 American Geophysical Union. All Rights Reserved.

Patsourakos, S., and M. K. Georgoulis, A Helicity-Based Method to Infer the CME Magnetic Field Magnitude in Sun and Geospace: Generalization and Extension to Sun-Like and M-Dwarf Stars and Implications for Exoplanet Habitability, *Solar Phys.*, *292*, 89, doi:10.1007/s11207-017-1124-1, 2017.

patsourakos, S., A. Vourlidas, and G. Stenborg, Direct Evidence for a Fast Coronal Mass Ejection Driven by the Prior Formation and Subsequent Destabilization of a Magnetic Flux Rope, *Astrophys. J.*, *764*, 125, doi:10.1088/0004-637X/764/2/125, 2013.

Patsourakos, S., et al., The Major Geoeffective Solar Eruptions of 2012 March 7: Comprehensive Sun-to-Earth Analysis, *Astrophys. J.*, *817*, 14, doi:10.3847/0004-637X/817/1/14, 2016.

Petrie, G., A. Pevtsov, A. Schwarz, and M. DeRosa, Modeling the Global Coronal Field with Simulated Synoptic Magnetograms from Earth and the Lagrange Points L_3, L_4, and L_5, *Sol. Phys.*, *293*, 88, doi:10.1007/s11207-018-1306-5, 2018.

Pinto, R. F., and A. S. Brun, Flux Emergence in a Magnetized Convection Zone, *Astrophys. J.*, *772*, 55, doi:10.1088/0004-637X/772/1/55, 2013.

Pinto, R. F., and A. P. Rouillard, A Multiple Flux-tube Solar Wind Model, *Astrophys. J.*, , *838*, 89, doi:10.3847/1538-4357/aa6398, 2017.

Pizzo, V., G. Millward, A. Parsons, D. Biesecker, S. Hill, and D. Odstrcil, Wang-Sheeley-Arge-Enlil Cone Model Transitions to Operations, *Space Weather*, *9*, 03004, doi:10.1029/2011SW000663, 2011.

Pizzo, V. J., C. de Koning, M. Cash, G. Millward, D. A. Biesecker, L. Puga, M. Codrescu, and D. Odstrcil, Theoretical basis for operational ensemble forecasting of coronal mass ejections, *Space Weather*, *13*, 676–697, doi:10.1002/2015SW001221, 2015.

©2019 American Geophysical Union. All Rights Reserved.

Accepted Article

Pomoell, J., and S. Poedts, EUHFORIA: European heliospheric forecasting information asset, *Journal of Space Weather and Space Climate*, *8*(27), A35, doi:10.1051/swsc/2018020, 2018.

Pomoell, J., E. Kilpua, C. Verbeke, E. Lumme, S. Poedts, E. Palmerio, and A. Isavnin, Modeling the Sun-To-Earth Evolution of the Magnetic Structure of Coronal Mass Ejections with EUHFORIA, in *EGU General Assembly Conference Abstracts*, *EGU General Assembly Conference Abstracts*, vol. 19, p. 11747, 2017.

Pulkkinen, A., Geomagnetically Induced Currents Modeling and Forecasting, *Space Weather*, *13*, 734–736, doi:10.1002/2015SW001316, 2015.

Pulkkinen, T., Space Weather: Terrestrial Perspective, *Living Reviews in Solar Physics*, *4*, 1, doi:10.12942/lrsp-2007-1, 2007.

Qian, L., and S. C. Solomon, Thermospheric Density: An Overview of Temporal and Spatial Variations, *Space Sci. Rev.*, *168*, 147–173, doi:10.1007/s11214-011-9810-z, 2012.

Qiu, J., Q. Hu, T. A. Howard, and V. B. Yurchyshyn, On the Magnetic Flux Budget in Low-Corona Magnetic Reconnection and Interplanetary Coronal Mass Ejections, *Astrophys. J.*, *659*, 758–772, doi:10.1086/512060, 2007.

Richardson, I. G., and H. V. Cane, Near-Earth Interplanetary Coronal Mass Ejections During Solar Cycle 23 (1996 - 2009): Catalog and Summary of Properties, *Sol. Phys.*, *264*, 189–237, doi:10.1007/s11207-010-9568-6, 2010.

Richardson, I. G., and H. V. Cane, Near-earth solar wind flows and related geomagnetic activity during more than four solar cycles (1963-2011), *Journal of Space Weather and Space Climate*, *2*(27), A02, doi:10.1051/swsc/2012003, 2012.

Accepted Article

©2019 American Geophysical Union. All Rights Reserved.

Riley, P., and N. U. Crooker, Kinematic Treatment of Coronal Mass Ejection Evolution in the Solar Wind, *Astrophys. J.*, *600*, 1035–1042, doi:10.1086/379974, 2004.

Riley, P., J. A. Linker, and Z. Mikić, An empirically-driven global MHD model of the solar corona and inner heliosphere, *J. Geophys. Res.,* , *106*, 15,889–15,902, doi:10.1029/2000JA000121, 2001.

Riley, P., M. Ben-Nun, J. A. Linker, M. J. Owens, and T. S. Horbury, Forecasting the properties of the solar wind using simple pattern recognition, *Space Weather*, *15*, 526–540, doi:10.1002/2016SW001589, 2017.

Riley, P., D. Baker, Y. D. Liu, P. Verronen, H. Singer, and M. Güdel, Extreme Space Weather Events: From Cradle to Grave, *Space Sci. Rev.*, *214*, 21, doi:10.1007/s11214-017-0456-3, 2018a.

Riley, P., et al., Forecasting the Arrival Time of Coronal Mass Ejections: Analysis of the CCMC CME Scoreboard, *Space Weather*, *16*, 1245–1260, doi:10.1029/2018SW001962, 2018b.

Ritter, B., et al., A Space weather information service based upon remote and in-situ measurements of coronal mass ejections heading for Earth. A concept mission consisting of six spacecraft in a heliocentric orbit at 0.72 AU, *Journal of Space Weather and Space Climate*, *5*(27), A3, doi:10.1051/swsc/2015006, 2015.

Robbrecht, E., S. Patsourakos, and A. Vourlidas, No Trace Left Behind: STEREO Observation of a Coronal Mass Ejection Without Low Coronal Signatures, *Astrophys. J.*, *701*, 283–291, doi:10.1088/0004-637X/701/1/283, 2009.

Rouillard, A. P., et al., Deriving the Properties of Coronal Pressure Fronts in 3D: Application to the 2012 May 17 Ground Level Enhancement, *Astrophys. J.*, *833*, 45, doi:

©2019 American Geophysical Union. All Rights Reserved.

Accepted Article

10.3847/1538-4357/833/1/45, 2016.

Roussev, I. I., K. Galsgaard, C. Downs, N. Lugaz, I. V. Sokolov, E. Moise, and J. Lin, Explaining fast ejections of plasma and exotic X-ray emission from the solar corona, *Nature Physics*, *8*, 845–849, doi:10.1038/nphys2427, 2012.

Ruffenach, A., et al., Statistical study of magnetic cloud erosion by magnetic reconnection, *Journal of Geophysical Research (Space Physics)*, *120*, 43–60, doi:10.1002/2014JA020628, 2015.

Salman, L. N. F. C. J. W. R. M. G. A. B. S. N. A., T. M., Forecasting periods of strong southward magnetic field following interplanetary shocks, *Space Weather*, 2018.

Savani, N. P., A. P. Rouillard, J. A. Davies, M. J. Owens, R. J. Forsyth, C. J. Davis, and R. A. Harrison, The radial width of a Coronal Mass Ejection between 0.1 and 0.4 AU estimated from the Heliospheric Imager on STEREO, *Annales Geophysicae*, *27*, 4349–4358, doi:10.5194/angeo-27-4349-2009, 2009.

Savani, N. P., A. Vourlidas, A. Szabo, M. L. Mays, I. G. Richardson, B. J. Thompson, A. Pulkkinen, R. Evans, and T. Nieves-Chinchilla, Predicting the magnetic vectors within coronal mass ejections arriving at Earth: 1. Initial architecture, *Space Weather*, *13*, 374–385, doi:10.1002/2015SW001171, 2015.

Savani, N. P., A. Vourlidas, I. G. Richardson, A. Szabo, B. J. Thompson, A. Pulkkinen, M. L. Mays, T. Nieves-Chinchilla, and V. Bothmer, Predicting the magnetic vectors within coronal mass ejections arriving at Earth: 2. Geomagnetic response, *Space Weather*, *15*, 441–461, doi:10.1002/2016SW001458, 2017.

Savcheva, A., N. Lugaz, B. van der Holst, R. Evans, and J. Zhang, Data-Constrined Simulations of CME eruption, in *Solar Heliospheric and INterplanetary Environment*

Accepted Article

©2019 American Geophysical Union. All Rights Reserved.

(SHINE 2017), p. 33, 2017.

Schrijver, C. J., et al., Understanding space weather to shield society: A global road map for 2015-2025 commissioned by COSPAR and ILWS, *Advances in Space Research*, *55*, 2745–2807, doi:10.1016/j.asr.2015.03.023, 2015.

Schwenn, R., A. dal Lago, E. Huttunen, and W. D. Gonzalez, The association of coronal mass ejections with their effects near the Earth, *Annales Geophysicae*, *23*, 1033–1059, doi:10.5194/angeo-23-1033-2005, 2005.

Scolini, C., C. Verbeke, S. Poedts, E. Chané, J. Pomoell, and F. P. Zuccarello, Effect of the Initial Shape of Coronal Mass Ejections on 3-D MHD Simulations and Geoeffectiveness Predictions, *Space Weather*, *16*, 754–771, doi:10.1029/2018SW001806, 2018.

Shen, C., Y. Wang, Z. Pan, M. Zhang, P. Ye, and S. Wang, Full halo coronal mass ejections: Do we need to correct the projection effect in terms of velocity?, *Journal of Geophysical Research (Space Physics)*, *118*, 6858–6865, doi:10.1002/2013JA018872, 2013.

Shiota, D., and R. Kataoka, Magnetohydrodynamic simulation of interplanetary propagation of multiple coronal mass ejections with internal magnetic flux rope (SUSANOO-CME), *Space Weather*, *14*, 56–75, doi:10.1002/2015SW001308, 2016.

Shiota, D., K. Kusano, T. Miyoshi, and K. Shibata, Magnetohydrodynamic Modeling for a Formation Process of Coronal Mass Ejections: Interaction Between an Ejecting Flux Rope and an Ambient Field, *Astrophys. J.*, *718*, 1305–1314, doi:10.1088/0004-637X/718/2/1305, 2010.

Taktakishvili, A., M. Kuznetsova, P. MacNeice, M. Hesse, L. Rastätter, A. Pulkkinen, A. Chulaki, and D. Odstrcil, Validation of the coronal mass ejection predictions at the

Accepted Article

©2019 American Geophysical Union. All Rights Reserved.

Earth orbit estimated by ENLIL heliosphere cone model, *Space Weather*, *7*, S03004, doi:10.1029/2008SW000448, 2009.

Temmer, M., A. M. Veronig, B. Vršnak, J. Rybák, P. Gömöry, S. Stoiser, and D. Maričić, Acceleration in Fast Halo CMEs and Synchronized Flare HXR Bursts, *ApJ Letters*, *673*, L95, doi:10.1086/527414, 2008.

Temmer, M., T. Rollett, C. Möstl, A. M. Veronig, B. Vršnak, and D. Odstrčil, Influence of the Ambient Solar Wind Flow on the Propagation Behavior of Interplanetary Coronal Mass Ejections, *Astrophys. J.*, *743*, 101, doi:10.1088/0004-637X/743/2/101, 2011a.

Temmer, M., A. M. Veronig, N. Gopalswamy, and S. Yashiro, Relation Between the 3D-Geometry of the Coronal Wave and Associated CME During the 26 April 2008 Event, *Solar Phys.*, *273*, 421–432, doi:10.1007/s11207-011-9746-1, 2011b.

Temmer, M., J. K. Thalmann, K. Dissauer, A. M. Veronig, J. Tschernitz, J. Hinterreiter, and L. Rodriguez, On Flare-CME Characteristics from Sun to Earth Combining Remote-Sensing Image Data with In Situ Measurements Supported by Modeling, *Solar Phys.*, *292*, 93, doi:10.1007/s11207-017-1112-5, 2017.

Temmer, M., et al., Characteristics of Kinematics of a Coronal Mass Ejection during the 2010 August 1 CME-CME Interaction Event, *Astrophys. J.*, *749*, 57, doi:10.1088/0004-637X/749/1/57, 2012.

Thernisien, A., A. Vourlidas, and R. A. Howard, Forward Modeling of Coronal Mass Ejections Using STEREO/SECCHI Data, *Sol. Phys.*, *256*, 111–130, doi:10.1007/s11207-009-9346-5, 2009.

Thernisien, A. F. R., R. A. Howard, and A. Vourlidas, Modeling of Flux Rope Coronal Mass Ejections, *Astrophys. J.*, *652*, 763–773, doi:10.1086/508254, 2006.

Accepted Article

©2019 American Geophysical Union. All Rights Reserved.

Thompson, W. T., B. Kliem, and T. Török, 3D Reconstruction of a Rotating Erupting Prominence, *Sol. Phys.*, *276*, 241–259, doi:10.1007/s11207-011-9868-5, 2012.

Titov, V. S., and P. Démoulin, Basic topology of twisted magnetic configurations in solar flares, *Astron. Astrophys.*, *351*, 707–720, 1999.

Titov, V. S., T. Török, Z. Mikic, and J. A. Linker, A Method for Embedding Circular Force-free Flux Ropes in Potential Magnetic Fields, *Astrophys. J.*, *790*, 163, doi:10.1088/0004-637X/790/2/163, 2014.

Tomczyk, S., et al., An Instrument to Measure Coronal Emission Line Polarization, *Sol. Phys.*, *247*, 411–428, doi:10.1007/s11207-007-9103-6, 2008.

Tomczyk, S., et al., Scientific objectives and capabilities of the Coronal Solar Magnetism Observatory, *Journal of Geophysical Research (Space Physics)*, *121*, 7470–7487, doi:10.1002/2016JA022871, 2016.

Törmä, O., *Laser communication concept for space weather forecasting CubeSat fleet mission*, 2016.

Török, T., B. Kliem, and V. S. Titov, Ideal kink instability of a magnetic loop equilibrium, *Astronom. and Astrophys.*, *413*, L27–L30, doi:10.1051/0004-6361:20031691, 2004.

Török, T., C. Downs, J. A. Linker, R. Lionello, V. S. Titov, Z. Mikić, P. Riley, R. M. Caplan, and J. Wijaya, Sun-to-Earth MHD Simulation of the 2000 July 14 "Bastille Day" Eruption, *Astrophys. J.*, *856*, 75, doi:10.3847/1538-4357/aab36d, 2018.

Tóth, G., et al., Extended magnetohydrodynamics with embedded particle-in-cell simulation of Ganymede's magnetosphere, *Journal of Geophysical Research (Space Physics)*, *121*, 1273–1293, doi:10.1002/2015JA021997, 2016.

Accepted Article

©2019 American Geophysical Union. All Rights Reserved.

Tschernitz, J., A. M. Veronig, J. K. Thalmann, J. Hinterreiter, and W. Pötzi, Reconnection Fluxes in Eruptive and Confined Flares and Implications for Superflares on the Sun, *Astrophys. J.*, *853*, 41, doi:10.3847/1538-4357/aaa199, 2018.

Tsurutani, B. T., W. D. Gonzalez, F. Tang, and Y. T. Lee, Great magnetic storms, *Geophys. Res. Lett.*, *19*, 73–76, doi:10.1029/91GL02783, 1992.

Tsurutani, B. T., W. D. Gonzalez, G. S. Lakhina, and S. Alex, The extreme magnetic storm of 1-2 September 1859, *Journal of Geophysical Research (Space Physics)*, *108*, 1268, doi:10.1029/2002JA009504, 2003.

Tsurutani, B. T., W. D. Gonzalez, X.-Y. Zhou, R. P. Lepping, and V. Bothmer, Properties of slow magnetic clouds, *Journal of Atmospheric and Solar-Terrestrial Physics*, *66*, 147–151, doi:10.1016/j.jastp.2003.09.007, 2004.

Žic, T., B. Vršnak, and M. Temmer, Heliospheric Propagation of Coronal Mass Ejections: Drag-based Model Fitting, *Astrphys. J.*, *218*, 32, doi:10.1088/0067-0049/218/2/32, 2015.

van Ballegooijen, A. A., E. R. Priest, and D. H. Mackay, Mean Field Model for the Formation of Filament Channels on the Sun, *Astrophys. J.,* , *539*, 983–994, doi:10.1086/309265, 2000.

van der Holst, B., W. B. Manchester, R. A. Frazin, A. M. Vásquez, G. Tóth, and T. I. Gombosi, A Data-driven, Two-temperature Solar Wind Model with Alfvén Waves, *Astrophys. J.*, *725*, 1373–1383, doi:10.1088/0004-637X/725/1/1373, 2010.

van der Holst, B., I. V. Sokolov, X. Meng, M. Jin, W. B. Manchester, IV, G. Tóth, and T. I. Gombosi, Alfvén Wave Solar Model (AWSoM): Coronal Heating, *Astrophys. J.*, *782*, 81, doi:10.1088/0004-637X/782/2/81, 2014.

©2019 American Geophysical Union. All Rights Reserved.

Accepted Article

Vasyliunas, V. M., Theoretical models of magnetic field line merging. I, *Reviews of Geophysics and Space Physics*, *13*, 303–336, doi:10.1029/RG013i001p00303, 1975.

Verbeke, C., S. Poedts, J. Pomoell, and C. Scolini, Modeling Coronal Mass Ejections with EUHFORIA: A Parameter Study of a magnetized Flux Rope Model, in *42nd COSPAR Scientific Assembly*, *COSPAR Meeting*, vol. 42, pp. D2.3–24–18, 2018.

Vourlidas, A., Mission to the Sun-Earth L_5 Lagrangian Point: An Optimal Platform for Space Weather Research, *Space Weather*, *13*, 197–201, doi:10.1002/2015SW001173, 2015.

Vourlidas, A., R. Colaninno, T. Nieves-Chinchilla, and G. Stenborg, The First Observation of a Rapidly Rotating Coronal Mass Ejection in the Middle Corona, *ApJ Letters*, *733*, L23, doi:10.1088/2041-8205/733/2/L23, 2011.

Vourlidas, A., B. J. Lynch, R. A. Howard, and Y. Li, How Many CMEs Have Flux Ropes? Deciphering the Signatures of Shocks, Flux Ropes, and Prominences in Coronagraph Observations of CMEs, *Sol. Phys.*, *284*, 179–201, doi:10.1007/s11207-012-0084-8, 2013.

Vourlidas, A., L. A. Balmaceda, G. Stenborg, and A. Dal Lago, Multi-viewpoint Coronal Mass Ejection Catalog Based on STEREO COR2 Observations, *Astrophys J.*, *838*, 141, doi:10.3847/1538-4357/aa67f0, 2017.

Vršnak, B., Processes and mechanisms governing the initiation and propagation of CMEs, *Annales Geophysicae*, *26*, 3089–3101, doi:10.5194/angeo-26-3089-2008, 2008.

Vršnak, B., D. Ruždjak, D. Sudar, and N. Gopalswamy, Kinematics of coronal mass ejections between 2 and 30 solar radii. What can be learned about forces governing the eruption?, *Astron. Astrophys.*, *423*, 717–728, doi:10.1051/0004-6361:20047169, 2004.

Accepted Article

©2019 American Geophysical Union. All Rights Reserved.

Vršnak, B., D. Sudar, D. Ruždjak, and T. Žic, Projection effects in coronal mass ejections, *Astronom. Astrophys.*, *469*, 339–346, doi:10.1051/0004-6361:20077175, 2007.

Wang, Y., C. Chen, B. Gui, C. Shen, P. Ye, and S. Wang, Statistical study of coronal mass ejection source locations: Understanding CMEs viewed in coronagraphs, *Journal of Geophysical Research (Space Physics)*, *116*, A04104, doi:10.1029/2010JA016101, 2011.

Wang, Y., B. Wang, C. Shen, F. Shen, and N. Lugaz, Deflected propagation of a coronal mass ejection from the corona to interplanetary space, *Journal of Geophysical Research (Space Physics)*, *119*, 5117–5132, doi:10.1002/2013JA019537, 2014.

Wang, Y.-M., and N. R. Sheeley, Jr., Solar wind speed and coronal flux-tube expansion, *Astrophys. J.,* , *355*, 726–732, doi:10.1086/168805, 1990.

Wang, Y. M., P. Z. Ye, and S. Wang, Multiple magnetic clouds: Several examples during March-April 2001, *Journal of Geophysical Research (Space Physics)*, *108*, 1370, doi:10.1029/2003JA009850, 2003.

Webb, D. F., and T. A. Howard, Coronal Mass Ejections: Observations, *Living Reviews in Solar Physics*, *9*, 3, doi:10.12942/lrsp-2012-3, 2012.

Weinzierl, M., D. H. Mackay, A. R. Yeates, and A. A. Pevtsov, The Possible Impact of L5 Magnetograms on Non-potential Solar Coronal Magnetic Field Simulations, *Astrophys. J.*, *828*, 102, doi:10.3847/0004-637X/828/2/102, 2016.

Welsch, B. T., Flux Accretion and Coronal Mass Ejection Dynamics, *Sol. Phys.*, *293*, 113, doi:10.1007/s11207-018-1329-y, 2018.

Wiegelmann, T., and T. Sakurai, Solar Force-free Magnetic Fields, *Living Reviews in Solar Physics*, *9*, 5, doi:10.12942/lrsp-2012-5, 2012.

Accepted Article

©2019 American Geophysical Union. All Rights Reserved.

Wiegelmann, T., G. J. D. Petrie, and P. Riley, Coronal Magnetic Field Models, *Space Sci. Rev.*, *210*, 249–274, doi:10.1007/s11214-015-0178-3, 2017.

Winslow, R. M., N. Lugaz, N. A. Schwadron, C. J. Farrugia, W. Yu, J. M. Raines, M. L. Mays, A. B. Galvin, and T. H. Zurbuchen, Longitudinal conjunction between MESSENGER and STEREO A: Development of ICME complexity through stream interactions, *Journal of Geophysical Research (Space Physics)*, *121*, 6092–6106, doi: 10.1002/2015JA022307, 2016.

Wold, A. M., M. L. Mays, A. Taktakishvili, L. K. Jian, D. Odstrcil, and P. MacNeice, Verification of real-time WSA-ENLIL+Cone simulations of CME arrival-time at the CCMC from 2010 to 2016, *Journal of Space Weather and Space Climate*, *8*, A17, doi: 10.1051/swsc/2018005, 2018.

Wu, S. T., M. Dryer, and S. M. Han, Interplanetary disturbances in the solar wind produced by density, temperature, or velocity pulses at 0.08 AU, *Sol. Phys.*, *49*, 187–204, doi:10.1007/BF00221493, 1976.

Xie, H., L. Ofman, and G. Lawrence, Cone model for halo CMEs: Application to space weather forecasting, *J. Geophys. Res.*, *109*, 3109–+, doi:10.1029/2003JA010226, 2004.

Xie, H., N. Gopalswamy, P. K. Manoharan, A. Lara, S. Yashiro, and S. Lepri, Long-lived geomagnetic storms and coronal mass ejections, *Journal of Geophysical Research (Space Physics)*, *111*, A01103, doi:10.1029/2005JA011287, 2006.

Xiong, M., J. A. Davies, B. Li, L. Yang, Y. D. Liu, L. Xia, R. A. Harrison, H. Keiji, and H. Li, Prospective Out-of-ecliptic White-light Imaging of Interplanetary Corotating Interaction Regions at Solar Maximum, *Astrophys. J.*, *844*, 76, doi:10.3847/1538-4357/aa7aaa, 2017.

Accepted Article

©2019 American Geophysical Union. All Rights Reserved.

Xue, X. H., C. B. Wang, and X. K. Dou, An ice-cream cone model for coronal mass ejections, *Journal of Geophysical Research (Space Physics)*, *110*, A08103, doi:10.1029/2004JA010698, 2005.

Yang, W. H., P. A. Sturrock, and S. K. Antiochos, Force-free magnetic fields - The magneto-frictional method, *Astrophys. J.*, *309*, 383–391, doi:10.1086/164610, 1986.

Yang, Y., F. Shen, Z. Yang, and X. Feng, Prediction of Solar Wind Speed at 1 AU Using an Artificial Neural Network, *Space Weather*, *16*, 1227–1244, doi:10.1029/2018SW001955, 2018.

Yardley, S. L., D. H. Mackay, and L. M. Green, Simulating the Coronal Evolution of AR 11437 Using SDO/HMI Magnetograms, *Astrophys. J.*, *852*, 82, doi:10.3847/1538-4357/aa9f20, 2018.

Yashiro, S., N. Gopalswamy, G. Michalek, O. C. St. Cyr, S. P. Plunkett, N. B. Rich, and R. A. Howard, A catalog of white light coronal mass ejections observed by the SOHO spacecraft, *Journal of Geophysical Research (Space Physics)*, *109*, A07105, doi:10.1029/2003JA010282, 2004.

Yurchyshyn, V., Q. Hu, R. P. Lepping, B. J. Lynch, and J. Krall, Orientations of LASCO Halo CMEs and their connection to the flux rope structure of interplanetary CMEs, *Advances in Space Research*, *40*, 1821–1826, doi:10.1016/j.asr.2007.01.059, 2007.

Yurchyshyn, V. B., H. Wang, P. R. Goode, and Y. Deng, Orientation of the Magnetic Fields in Interplanetary Flux Ropes and Solar Filaments, *Astrophys. J.*, *563*, 381–388, doi:10.1086/323778, 2001.

Zhang, J., K. P. Dere, R. A. Howard, M. R. Kundu, and S. M. White, On the Temporal Relationship between Coronal Mass Ejections and Flares, *Astrophys. J.*, *559*, 452–462,

Accepted Article

©2019 American Geophysical Union. All Rights Reserved.

doi:10.1086/322405, 2001.

Zhang, J., X. Cheng, and M.-D. Ding, Observation of an evolving magnetic flux rope before and during a solar eruption, *Nature Communications*, *3*, 747, doi:10.1038/ncomms1753, 2012.

Zhang, J., et al., Solar and interplanetary sources of major geomagnetic storms (Dst < -100 nT) during 1996-2005, *Journal of Geophysical Research (Space Physics)*, *112*, A10102, doi:10.1029/2007JA012321, 2007.

Zheng, Y., et al., Forecasting propagation and evolution of CMEs in an operational setting: What has been learned, *Space Weather*, *11*, 557–574, doi:10.1002/swe.20096, 2013.

Zuccarello, F. P., D. B. Seaton, M. Mierla, S. Poedts, L. A. Rachmeler, P. Romano, and F. Zuccarello, Observational Evidence of Torus Instability as Trigger Mechanism for Coronal Mass Ejections: The 2011 August 4 Filament Eruption, *Astrophys. J.*, *785*, 88, doi:10.1088/0004-637X/785/2/88, 2014.

Zurbuchen, T. H., and I. G. Richardson, In-Situ Solar Wind and Magnetic Field Signatures of Interplanetary Coronal Mass Ejections, *Space Sci. Rev.*, *123*, 31–43, doi:10.1007/s11214-006-9010-4, 2006.

Accepted Article

©2019 American Geophysical Union. All Rights Reserved.

Accepted Article

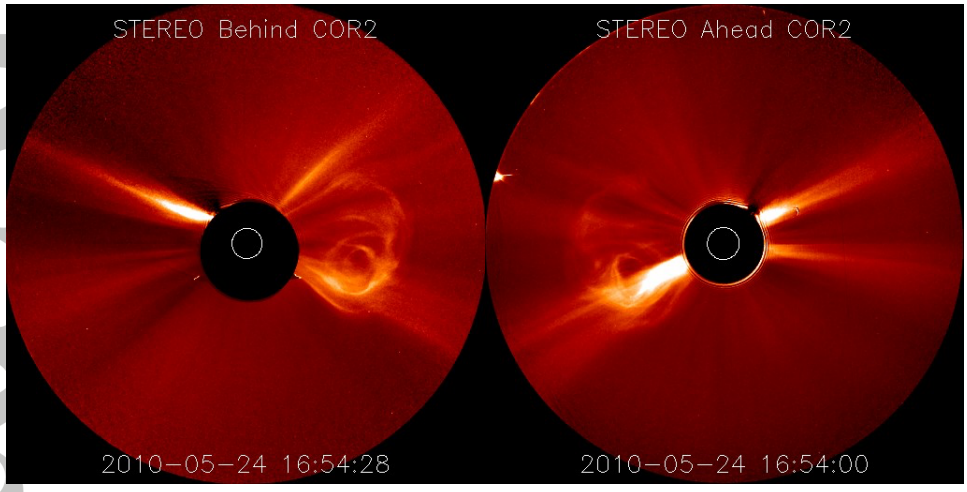

Figure 1. A CME on May 24, 2010 seen by two STEREO spacecraft separated by about 120 degrees in longitude; left) STEREO-A/COR2 and right) STEREO-B/COR2.

©2019 American Geophysical Union. All Rights Reserved.

Accepted Article

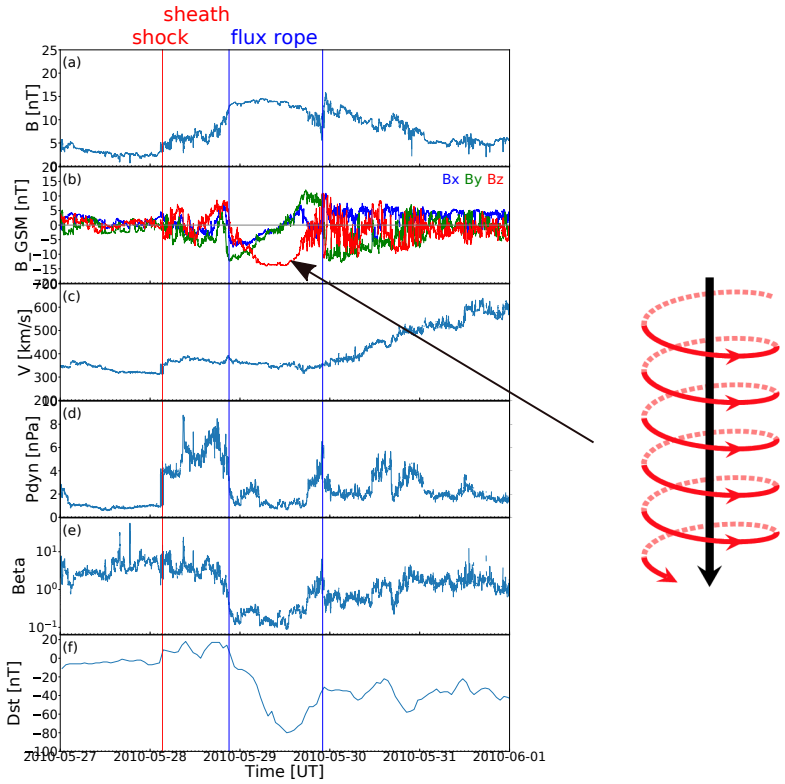

Figure 2. An ICME observed in the near Earth solar wind during May 28-29, 2010. The data are from the OMNI database. The panels give: a) magnetic field magnitude, b) magnetic field components in GSM coordinate system, c) solar wind speed, d) solar wind dynamic pressure, e) solar wind plasma beta (i.e., the ratio of the plasma pressure to the magnetic pressure), and f) 1-hour Dst index. The red line shows the shock and the ICME flux rope is between the pair of blue lines. The schematic on right (from *Palmerio et al.* [2018]) illustrates the local variations of the magnetic field around the axis of the flux rope.

©2019 American Geophysical Union. All Rights Reserved.

Accepted Article

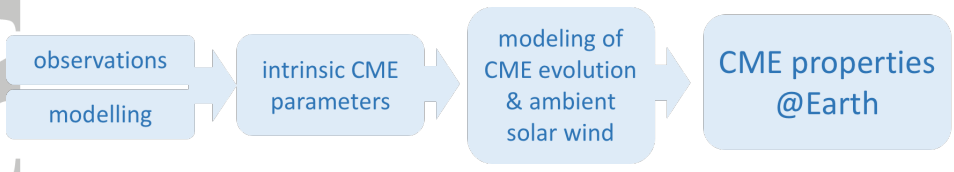

Figure 3. The forecasting chain to derive CME properties at Earth. The intrinsic CME parameters are obtained from remote-sensing observations and/or modeling which are then fed into the models covering coronal and/or heliospheric models. Models need to cover the background solar wind in which the CME is propagating as well as the CME evolution itself. Both aspects are closely interlinked.

©2019 American Geophysical Union. All Rights Reserved.

Accepted Article

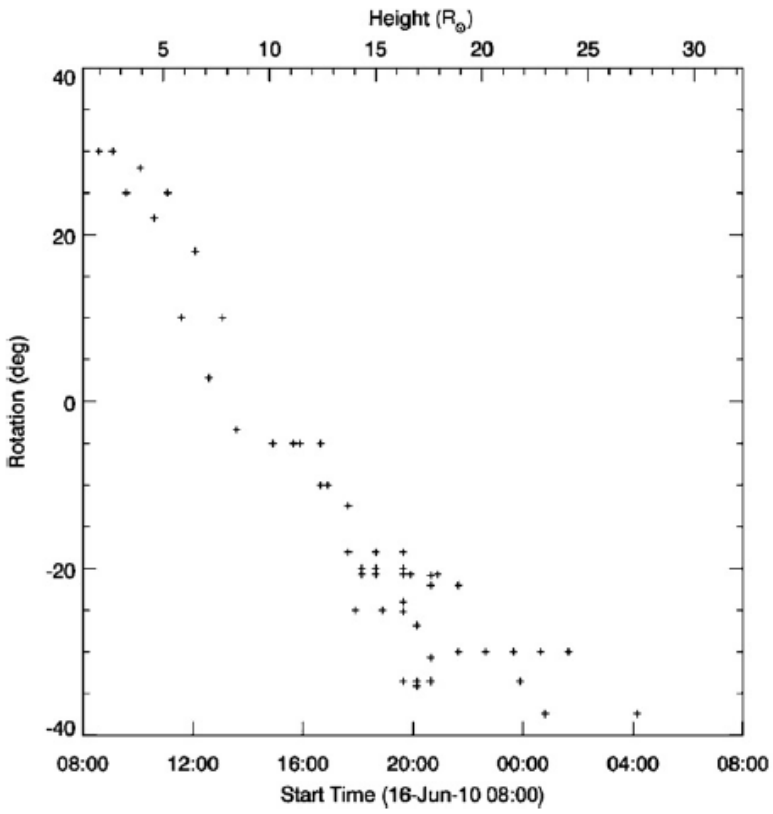

Figure 4. Rotation angle of a CME as a function of time. The radial distance from the Sun is given at top. The amount of rotation is obtained from applying a forward-fitting model to STEREO and LASCO coronagraph images. Figure is taken from *Vourlidas et al.* [2011].

©2019 American Geophysical Union. All Rights Reserved.

Accepted Article

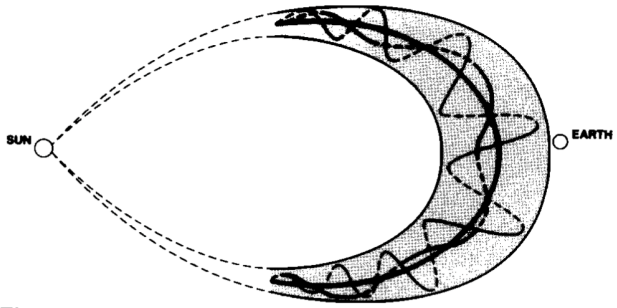

Figure 5. A schematic of an interplanetary CME (ICME) consisting of a huge bent flux rope loop. From *Burlaga et al.* [1990].

©2019 American Geophysical Union. All Rights Reserved.

Accepted Article

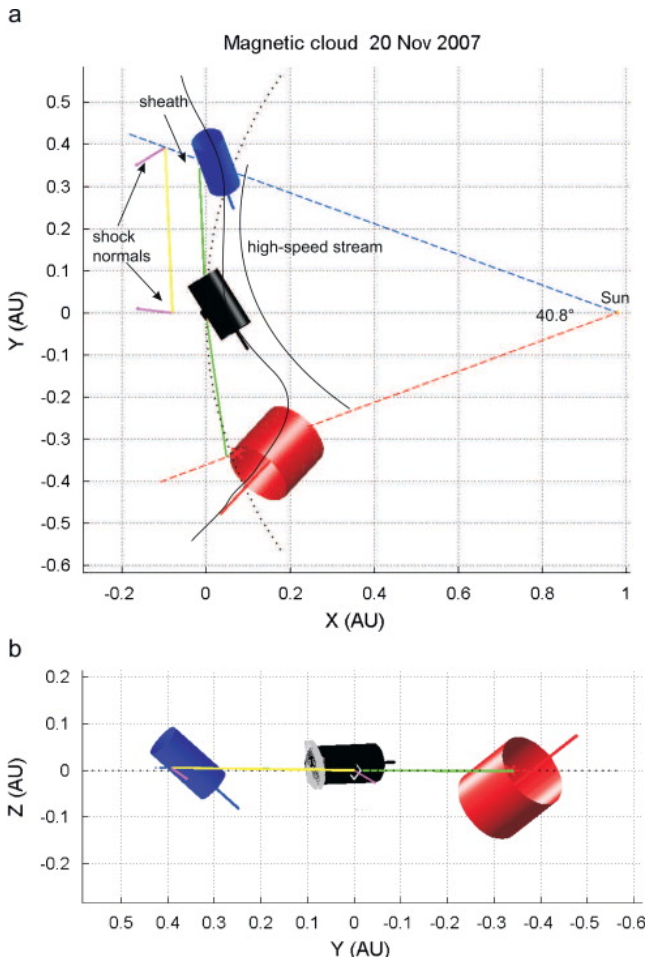

Figure 6. Illustration of flux rope orientations and sizes at three locations (STEREO-A, L1, and STEREO-B) during a flux rope ICME detected on November 19–20, 2007. The blue cylinder shows flux rope at STEREO-B, black at L1 (Wind) and red at STEREO-A. The coordinates are solar ecliptic coordinate system. From *Farrugia et al.* [2011].

©2019 American Geophysical Union. All Rights Reserved.

Accepted Article

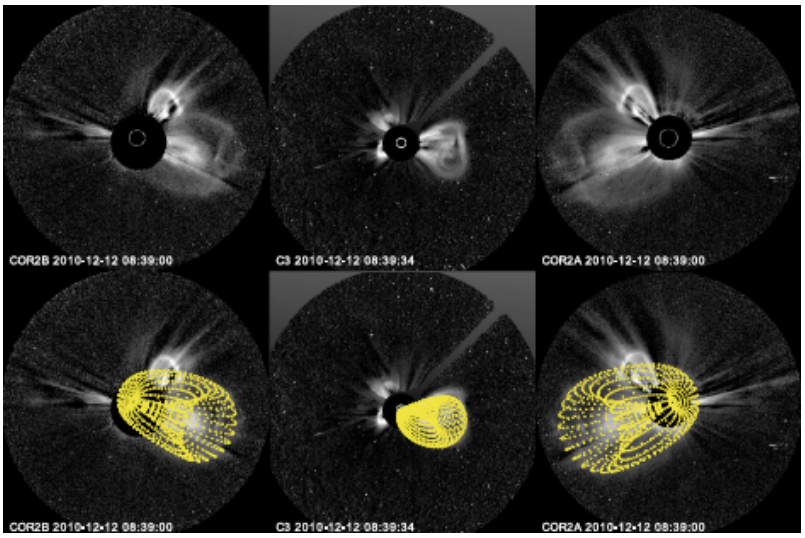

Figure 7. Forward modeling of a CME using observations from three widely separated spacecraft (SOHO, STEREO-A and STEREO-B, each separated from each other by about 120°). The yellow wireframe in the bottom panel shows the result of the fit. Figure is taken from *Isavnin* [2016].

©2019 American Geophysical Union. All Rights Reserved.

Accepted Article

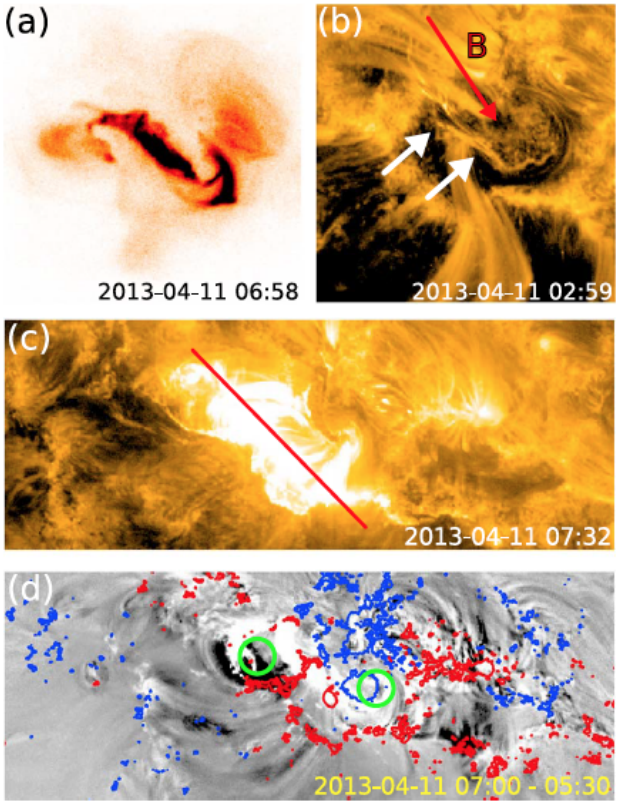

Figure 8. Estimating the magnetic field structure of CMEs by combining different indirect proxies. LH (a) Reverse S-shaped sigmoid seen from Hinode/X-Ray Telescope (b) Filament threads (white arrows) from SDO/AIA 171 . The red shows the direction of the magnetic field along the filament axis. (c) Post-eruptive arcades from SDO/AIA 171 and their approximate orientation indicated with a red arrow. (d) Base-difference SDO/AIA image at 211Å overlaid with SDO/HMI magnetogram (blue shows negative polarity and red positive polarity). This panel also shows reverse J-shaped flare ribbons. All chirality proxies suggest left-handed helicity for the flux rope. Figure is taken from Palmerio et al. (2018).

©2019 American Geophysical Union. All Rights Reserved.

Accepted Article

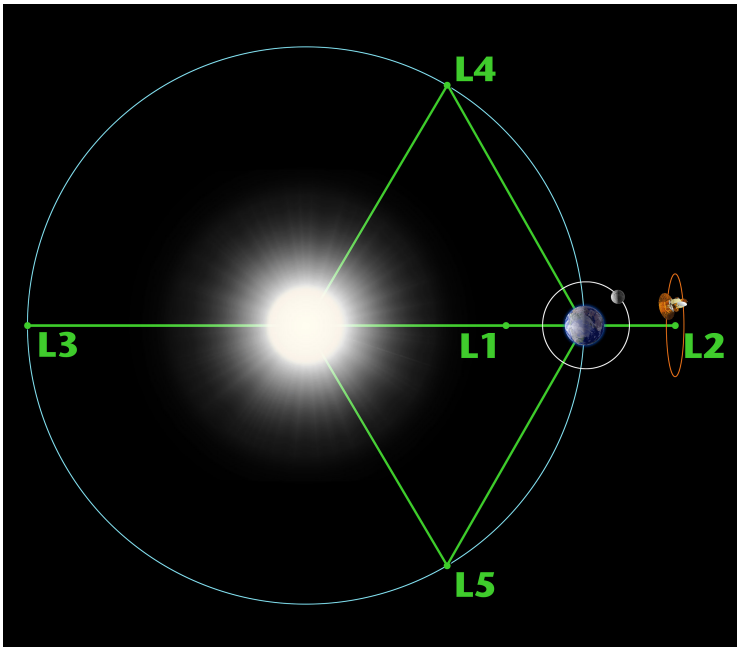

Figure 9. Lagrangian points. Source: NASA/WMAP Science Team.

©2019 American Geophysical Union. All Rights Reserved.

Accepted Article

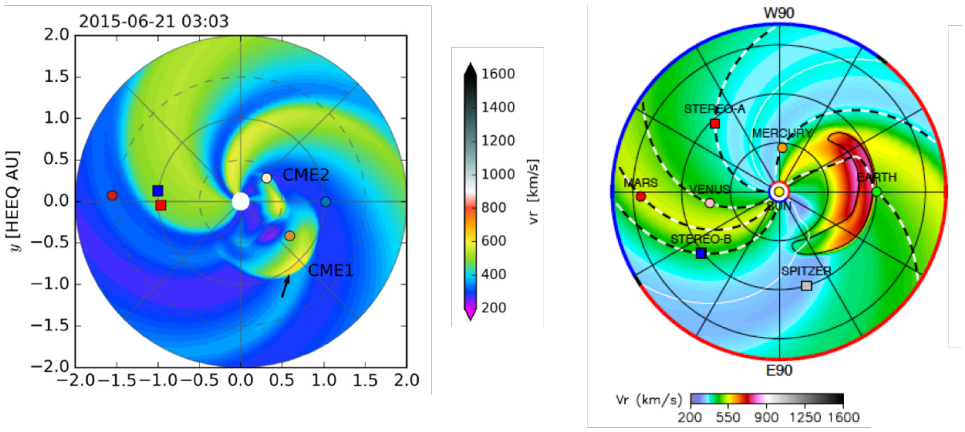

Figure 10. Snapshots showing a global view of CME modelled with a) EUHFORIA for June 21, 2015 [*Pomoell and Poedts*, 2018] and b) ENLIL for April 13, 2013 [*Mays et al.*, 2015a]. The parameter shown in the plot is the radial velocity. Circles and squares show the position of the planets and spacecraft in the inner heliosphere.

©2019 American Geophysical Union. All Rights Reserved.

Accepted Article

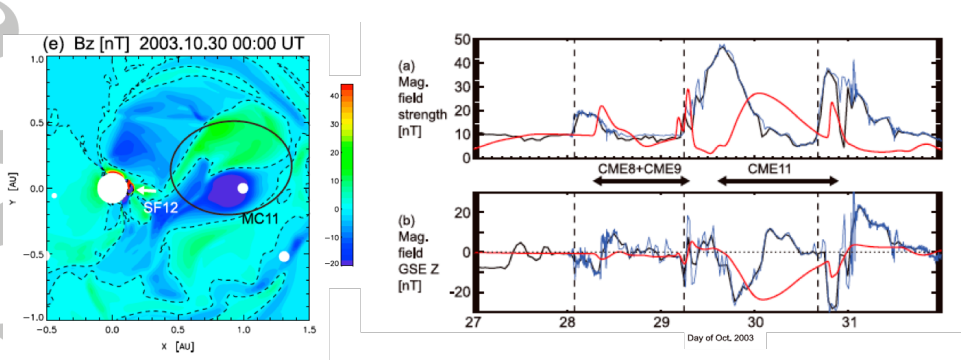

Figure 11. Results of the SUSANOO-CME run for CMEs observed during October 27-31, 2013. The left panel shows the distribution of the magnetic field north-south component (B_Z) in GSE coordinates. The right panel shows the model prediction (red) of the magnetic field magnitude and B_Z and comparision to ACE measurements (red) from the Lagrangian point L1. The dashed lines show the times of interplanetary shocks. The picture is from *Shiota and Kataoka* [2016].

©2019 American Geophysical Union. All Rights Reserved.